

NASA TECHNICAL NOTE



NASA TN D-5857

NASA TN D-5857

**CASE FILE  
COPY**

FULL-SCALE WIND-TUNNEL INVESTIGATION  
OF THE STATIC LONGITUDINAL  
AND LATERAL CHARACTERISTICS OF A  
LIGHT SINGLE-ENGINE LOW-WING AIRPLANE

*by James P. Shivers, Marvin P. Fink,  
and George M. Ware*

*Langley Research Center  
Hampton, Va. 23365*



1. Report No. NASA TN D-5857	2. Government Accession No.	3. Recipient's Catalog No.	
4. Title and Subtitle FULL-SCALE WIND-TUNNEL INVESTIGATION OF THE STATIC LONGITUDINAL AND LATERAL CHARACTERISTICS OF A LIGHT SINGLE-ENGINE LOW-WING AIRPLANE		5. Report Date June 1970	6. Performing Organization Code
		8. Performing Organization Report No. L-7121	10. Work Unit No. 736-01-10-01
7. Author(s) James P. Shivers, Marvin P. Fink, and George M. Ware		11. Contract or Grant No.	
		13. Type of Report and Period Covered Technical Note	
9. Performing Organization Name and Address NASA Langley Research Center Hampton, Va. 23365		14. Sponsoring Agency Code	
		12. Sponsoring Agency Name and Address National Aeronautics and Space Administration Washington, D.C. 20546	
15. Supplementary Notes			
16. Abstract  The airplane was a light single-engine low-wing monoplane. Tests were made for an angle-of-attack range of $-4^{\circ}$ to $22^{\circ}$ and over a sideslip range from $15^{\circ}$ to $-15^{\circ}$ at thrust coefficients of approximately 0.03 and 0.23. Control effectiveness was determined for a full range of deflections on the aileron, elevator, rudder, and flap.			
17. Key Words (Suggested by Author(s))  Light single-engine airplane Stability and control		18. Distribution Statement  Unclassified - Unlimited	
19. Security Classif. (of this report) Unclassified	20. Security Classif. (of this page) Unclassified	21. No. of Pages 63	22. Price* \$3.00

\*For sale by the Clearinghouse for Federal Scientific and Technical Information  
Springfield, Virginia 22151



FULL-SCALE WIND-TUNNEL INVESTIGATION OF THE  
STATIC LONGITUDINAL AND LATERAL CHARACTERISTICS OF A  
LIGHT SINGLE-ENGINE LOW-WING AIRPLANE

By James P. Shivers, Marvin P. Fink, and George M. Ware  
Langley Research Center

SUMMARY

A wind-tunnel investigation has been conducted in the Langley full-scale tunnel to determine the static longitudinal and lateral stability and control characteristics of a light single-engine airplane. The investigation was made over an angle-of-attack range of  $-4^{\circ}$  to  $22^{\circ}$  at various angles of sideslip between  $15^{\circ}$  and  $-15^{\circ}$  for various power and flap settings. The power conditions were  $T'_c \approx 0.03$  which represents a cruise condition of about 70 percent power and  $T'_c \approx 0.23$  which corresponds to a full power climb condition (where  $T'_c$  is thrust coefficient).

The investigation showed that the airplane has stick-fixed longitudinal stability for angles of attack up to and through the stall for all configurations tested with the center of gravity at 0.25 mean aerodynamic chord. Power generally had a small destabilizing effect. The airplane is directionally stable and has positive effective dihedral through the stall for all test conditions. The aileron and rudder effectiveness was maintained through the stall and was powerful enough to trim out all airplane rolling and yawing moments through the stall.

INTRODUCTION

For the past several years the Flight Research Center has been conducting a program to evaluate the flying qualities of a number of general-aviation aircraft. The results of these investigations have been reported in reference 1. As a part of the continuing investigation, one of the airplanes investigated in reference 1, a light twin-engine configuration, was tested in the Langley full-scale tunnel, and the results given in reference 2. In addition, a single-engine version of the airplane of reference 2 was investigated and the results are reported in reference 3. The present investigation was made to determine the static longitudinal and lateral stability and control characteristics of another single-engine airplane of about the same gross weight as the airplane of reference 3 but with different geometric characteristics and airfoil. The investigation was made with various power and flap settings over a range of angle of attack from  $-4^{\circ}$  to  $22^{\circ}$

and over a range of sideslip angle from  $-15^{\circ}$  to  $15^{\circ}$ . The tests were made at a tunnel speed of about 93 feet per second (28.3 meters per second) giving a Reynolds number of approximately  $3.37 \times 10^6$ .

## SYMBOLS

The stability-axis system used in the presentation of the data and the positive direction of forces, moments, and angles are shown in figure 1. The data are computed about the moment center shown in figure 2 which is at 25 percent of the mean aerodynamic chord.

b	wing span, 33.38 feet (10.20 meters)
$C_D$	drag coefficient, $\frac{\text{Drag}}{qS}$
$C_L$	lift coefficient, $\frac{\text{Lift}}{qS}$
$C_Y$	side-force coefficient, $\frac{\text{Side force}}{qS}$
$C_l$	rolling-moment coefficient, $\frac{\text{Rolling moment}}{qSb}$
$C_{l\beta}$	lateral stability parameter (taken between $\pm 10^{\circ}$ $\beta$ ), $\frac{\partial C_l}{\partial \beta}$ , per degree
$C_{l\delta_a}$	aileron rolling-moment parameter, $\frac{\partial C_l}{\partial \delta_a}$ , per degree
$C_m$	pitching-moment coefficient, $\frac{\text{Pitching moment}}{qS\bar{c}}$
$C_{m\delta_e}$	elevator effectiveness parameter, $\frac{\partial C_m}{\partial \delta_e}$ , per degree
$\frac{\partial C_m}{\partial C_L}$	longitudinal stability parameter
$C_n$	yawing-moment coefficient, $\frac{\text{Yawing moment}}{qSb}$
$C_{n\beta}$	directional stability parameter (taken between $\pm 10^{\circ}$ $\beta$ ), $\frac{\partial C_n}{\partial \beta}$ , per degree
$C_{n\delta_a}$	aileron yawing-moment parameter, $\frac{\partial C_n}{\partial \delta_a}$ , per degree
$C_{n\delta_r}$	rudder effectiveness parameter, $\frac{\partial C_n}{\partial \delta_r}$ , per degree

$\bar{c}$	mean aerodynamic chord, 5.67 feet (1.73 meters)
$i_t$	horizontal tail incidence, positive trailing edge down, degrees
$q$	free-stream dynamic pressure, pounds per foot <sup>2</sup> (newtons per meter <sup>2</sup> )
$S$	wing area, 180 foot <sup>2</sup> (16.70 meter <sup>2</sup> )
$T$	effective thrust (at $\alpha = 0^\circ$ ), $\text{Drag}_{\text{propellers removed}} - \text{Drag}_{\text{propellers operating}}$
$T'_c$	thrust coefficient, $\frac{T}{qS}$
$V$	velocity, feet per second (meters per second)
$X, Y, Z$	stability axes
$\alpha$	angle of attack of fuselage reference line, degrees
$\beta$	angle of sideslip, positive nose to left, degrees
$\delta_a$	total aileron deflection, positive right aileron down, $\delta_{a,\text{left}} - \delta_{a,\text{right}}$ , degrees
$\delta_e$	elevator deflection, positive trailing edge down, degrees
$\delta_f$	flap deflection, positive trailing edge down, degrees
$\delta_r$	rudder deflection, positive trailing edge left, degrees

### AIRPLANE

The airplane tested was a light, single-engine, low-wing monoplane having a maximum take-off weight of 2750 lb (12 250 N). The principal dimensions are given in figure 2 and the airplane mounted in the tunnel test section is shown in figure 3. The airplane had a wing span of 33.38 ft (10.20 m), a wing area of 180 ft<sup>2</sup> (16.70 m<sup>2</sup>), an aspect ratio of 6.19, and a mean aerodynamic chord of 5.67 ft (1.73 m). The airfoil section for the wing was designated by the manufacturer as an NACA 4415R airfoil section at the root and an NACA 6410R airfoil at the tip. The wing had 3.0° of geometric twist (the

wing tip had  $3.0^\circ$  less incidence than the wing root), had  $7.5^\circ$  of dihedral, and was at  $2^\circ$  positive incidence with respect to the fuselage reference line. The thrust axis was parallel to the reference line. The airplane had a standard three-control system. The horizontal tail was of the stabilizer-elevator type with an elevator travel from  $20^\circ$  to  $-30^\circ$ . The stabilizer for this airplane is normally set at zero incidence, but for these tests, it was set at  $-5^\circ$  and  $+5^\circ$  incidence. The aileron travel was from  $20^\circ$  to  $-30^\circ$ , and the rudder travel was from  $-30^\circ$  to  $30^\circ$ . The vertical stabilizer was offset  $2^\circ$  to the left of the center line. The hinge line of the slotted trailing-edge flap was modified so that the flap hinge axis was in line with the aileron hinge line. For this investigation, the main landing gear was removed and the wheel wells covered with sheet metal. The nose gear was always retracted. Power was provided by a 266-hp (198 kW) variable-frequency electric motor.

## TESTS

The tests were made to determine the static longitudinal and lateral stability and control characteristics of the airplane for several flight conditions. The airplane was tested over an angle-of-attack range from  $-4^\circ$  to  $22^\circ$  and over a sideslip range from  $-15^\circ$  to  $15^\circ$  for  $0^\circ$ ,  $20^\circ$ , and  $30^\circ$  flap deflections. A range of elevator angle from  $17.9^\circ$  to  $-23.0^\circ$  was investigated at zero sideslip with  $-5^\circ$  tail incidence and from  $11.3^\circ$  to  $-30^\circ$  with  $5^\circ$  tail incidence. The two tail incidence settings were tested to provide information for estimating the average downwash angle at the tail. Rudder effectiveness was measured over the sideslip range. References 2 and 3 showed that aileron effectiveness was not appreciably affected by power, flap deflection, or sideslip. Consequently, in the present investigation, aileron effectiveness was measured only at zero sideslip and flap deflection for low and high thrust coefficients  $T'_C$  of approximately 0.03 and 0.23 which represent a cruise and a climb condition, respectively. A thrust coefficient of 0.20 would correspond to 600 pounds (2.67 kN) of thrust at a flight speed of 80 mph (35.7632 m/sec) which would be equivalent to approximately 200 hp (149 kW).

The test vehicle had a controllable pitch propeller on which blade angle and rotational speed was controlled and indicated remotely. The blade angle and advance ratio for a given thrust coefficient were determined and set for each test. However, a variation in instrumentation voltage which was not perceptible during the investigation resulted in a variation in propeller blade angle from test to test and caused deviations from the preselected thrust values. Once set, however, the blade angle remained constant over the angle-of-attack range. The actual thrust coefficient for each individual test was determined from data analysis and is indicated in the figures.

## PRESENTATION OF DATA

The data from these tests have been corrected for airstream misalignment, buoyancy effects, mounting strut tares, and wind-tunnel jet-boundary effects.

The data are presented in the following figures:

	Figure
Longitudinal aerodynamic characteristics with propeller removed . . . . .	4
Longitudinal aerodynamic characteristics with propeller removed and at low power with propeller on . . . . .	5
Longitudinal aerodynamic characteristics with power and for flap deflection, $i_t = -5^\circ$ . . . . .	6 to 8
Longitudinal aerodynamic characteristics with power and for flap deflection, $i_t = 5^\circ$ . . . . .	9 to 11
Longitudinal aerodynamic characteristics with horizontal tail removed . . . .	12
Variation of pitching-moment coefficient with elevator deflection . . . . .	13 and 14
Lateral stability and control characteristics with power and for flap deflection . . . . .	15 to 17
Lateral stability and control characteristics for aileron deflection . . . . .	18
Lateral stability and control characteristics for rudder deflection, $\delta_f = 0^\circ$ . . . . .	19
Lateral stability and control characteristics for rudder deflection, $\delta_f = 20^\circ$ . . . . .	20
Lateral stability and control characteristics for rudder deflection, $\delta_f = 30^\circ$ . . . . .	21
Effect of power on longitudinal aerodynamic characteristics . . . . .	22
Longitudinal stability . . . . .	23
Horizontal tail control power . . . . .	24
Effective dihedral and directional stability characteristics . . . . .	25
Aileron effectiveness . . . . .	26
Rudder effectiveness . . . . .	27
Comparison of rolling- and yawing-moment coefficients for various thrust coefficients and flap deflections . . . . .	28
Control capability for overcoming lateral moments . . . . .	29

## RESULTS AND DISCUSSION

The basic data obtained during the wind-tunnel investigation are presented in figures 4 to 21 without analysis. Summary plots have been prepared from some of these

data to illustrate the general static stability and control characteristics of the airplane. Only the summary plots are discussed.

### Longitudinal Aerodynamic Characteristics

The longitudinal aerodynamic characteristics of the airplane with various power conditions are presented in figure 22 for flap deflections of  $0^\circ$ ,  $20^\circ$ , and  $30^\circ$ . As might be expected, increasing power results in an increase in lift-curve slope and maximum lift coefficient because of the increased slipstream velocity over the wing.

The pitching-moment curves shown in figure 22 are virtually linear up to the stall and then exhibit a nose-down pitching moment at higher angles of attack. For a given flap deflection, increasing power generally has little effect on the pitching-moment characteristics except for a small trim change. Illustrated in figure 23 is the variation in static margin  $-\partial C_m / \partial C_L$  with lift coefficient for the various flap deflections and thrust coefficients. These data are a measure of the stick-fixed stability and show that power is slightly destabilizing.

The variation of elevator effectiveness with angle of attack at  $T'_C \approx 0.03$  and  $0.23$  is presented in figure 24 for flap deflections of  $0^\circ$ ,  $20^\circ$ , and  $30^\circ$ . These data show that the effectiveness remained nearly constant over the angle-of-attack range and that it was reduced slightly by flap deflection.

### Lateral Stability and Control Characteristics

The variation of the effective-dihedral parameter  $C_{l\beta}$  and directional stability parameter  $C_{n\beta}$  with angle of attack is shown in figure 25 for the several flap deflections and thrust coefficients. The data show that the airplane has positive effective dihedral ( $-C_{l\beta}$ ) in all conditions. The usual general reduction in the effective dihedral with increasing angle of attack up to about the stall angle took place except at low thrust coefficient and zero flap deflection. The effective dihedral was greatly reduced when the flaps were deflected.

The data of figure 25 also show that the airplane is directionally stable for all test conditions although there is some decrease in directional stability at the higher angles of attack and that deflecting the flaps causes a small reduction in stability with power on. Power caused an increase in the directional stability as would be expected because of the increase in dynamic pressure at the tail.

The variation of the aileron control characteristics  $C_{l\delta a}$  and  $C_{n\delta a}$  with angle of attack is presented in figure 26 for flap deflections of  $0^\circ$  and  $30^\circ$  and a low thrust coefficient. These data show that, in general, the rolling moment remains at a fairly constant level throughout the angle-of-attack range and is relatively unaffected by flap deflection.

However, the variation of the yawing moments with angle of attack show that the ailerons produce adverse yaw and the magnitude of the yawing moment increases with increasing angle of attack.

The variation of rudder effectiveness with angle of attack is presented in figure 27 for a low and a high thrust coefficient and for flap deflections of  $0^\circ$ ,  $20^\circ$ , and  $30^\circ$ . These data show that rudder effectiveness is maintained throughout the angle-of-attack range for all test conditions, and the effectiveness is appreciably increased with an increase in power because of the increased dynamic pressure at the tail caused by the slipstream.

The basic lateral trim characteristics of the airplane, as shown by the variation of the lateral coefficients  $C_l$  and  $C_n$  with angle of attack for  $0^\circ$  sideslip, are presented in figure 28 for the various flap deflections and thrust coefficients. The data show that below the stall there is an out-of-trim positive rolling moment that decreases with increasing angle of attack until, near the stall, the rolling moment becomes negative. These rolling moments, however, are not unusually large. It may be noted in figure 28 that power reduced the out-of-trim rolling moments that were present at the low power condition. This is opposite to the effect of power on the rolling moments of the airplane of reference 3. This difference may be due, in part, to the thrust axis of the airplane of reference 3 being offset  $3^\circ$  to the right and the vertical stabilizer of the airplane of the present investigation being offset  $2^\circ$  to the left. The data also show that the yawing moment is nearly zero at the low thrust setting since the vertical stabilizer is offset to trim the airplane near the cruise thrust coefficient ( $T'_c \approx 0.03$ ). The action of the slipstream on the vertical tail with increased thrust coefficient causes a negative yawing moment as might be expected.

An attempt has been made to determine whether the controls are powerful enough to overcome the asymmetric moments near the stall, and the results of the analysis are presented in figure 29. In this figure are plotted the variation of the rolling and yawing moments with angle of attack at  $0^\circ$  sideslip for  $T'_c \approx 0.03$  and  $\delta_f = 30^\circ$ . Added to these curves are the moments available from full aileron and rudder deflection at  $\delta_f = 0^\circ$  (including the adverse yaw of the ailerons and the roll due to rudder deflection). These data show that, based on static wind-tunnel results, the rolling and yawing moments available from aileron and rudder are more than adequate to overcome the out-of-trim moments of the airplane.

## CONCLUSIONS

A full-scale wind-tunnel investigation has been made to determine the static longitudinal and lateral stability and control characteristics of a second single-engine airplane. The following conclusions were drawn from the results of the investigation:

1. The airplane has stick-fixed longitudinal stability through the stall for all configurations tested with the center of gravity at 0.25 mean aerodynamic chord. Power generally has a small destabilizing effect but the airplane would be statically stable for all test conditions.

2. The airplane is directionally stable and has positive effective dihedral through the stall for all test conditions.

3. Aileron and rudder effectiveness is maintained through the stall.

4. Aileron and rudder controls are powerful enough to trim out all airplane rolling and yawing moments through the stall.

Langley Research Center,  
National Aeronautics and Space Administration,  
Hampton, Va., April 27, 1970.

#### REFERENCES

1. Barber, Marvin R.; Jones, Charles K.; Sisk, Thomas R.; and Haise, Fred W.: An Evaluation of the Handling Qualities of Seven General-Aviation Aircraft. NASA TN D-3726, 1966.
2. Fink, Marvin P.; and Freeman, Delma C., Jr.: Full-Scale Wind-Tunnel Investigation of Static Longitudinal and Lateral Characteristics of a Light Twin-Engine Airplane. NASA TN D-4983, 1969.
3. Fink, Marvin P.; Freeman, Delma C., Jr.; and Greer, H. Douglas: Full-Scale Wind-Tunnel Investigation of the Static Longitudinal and Lateral Characteristics of a Light Single-Engine Airplane. NASA TN D-5700, 1970.

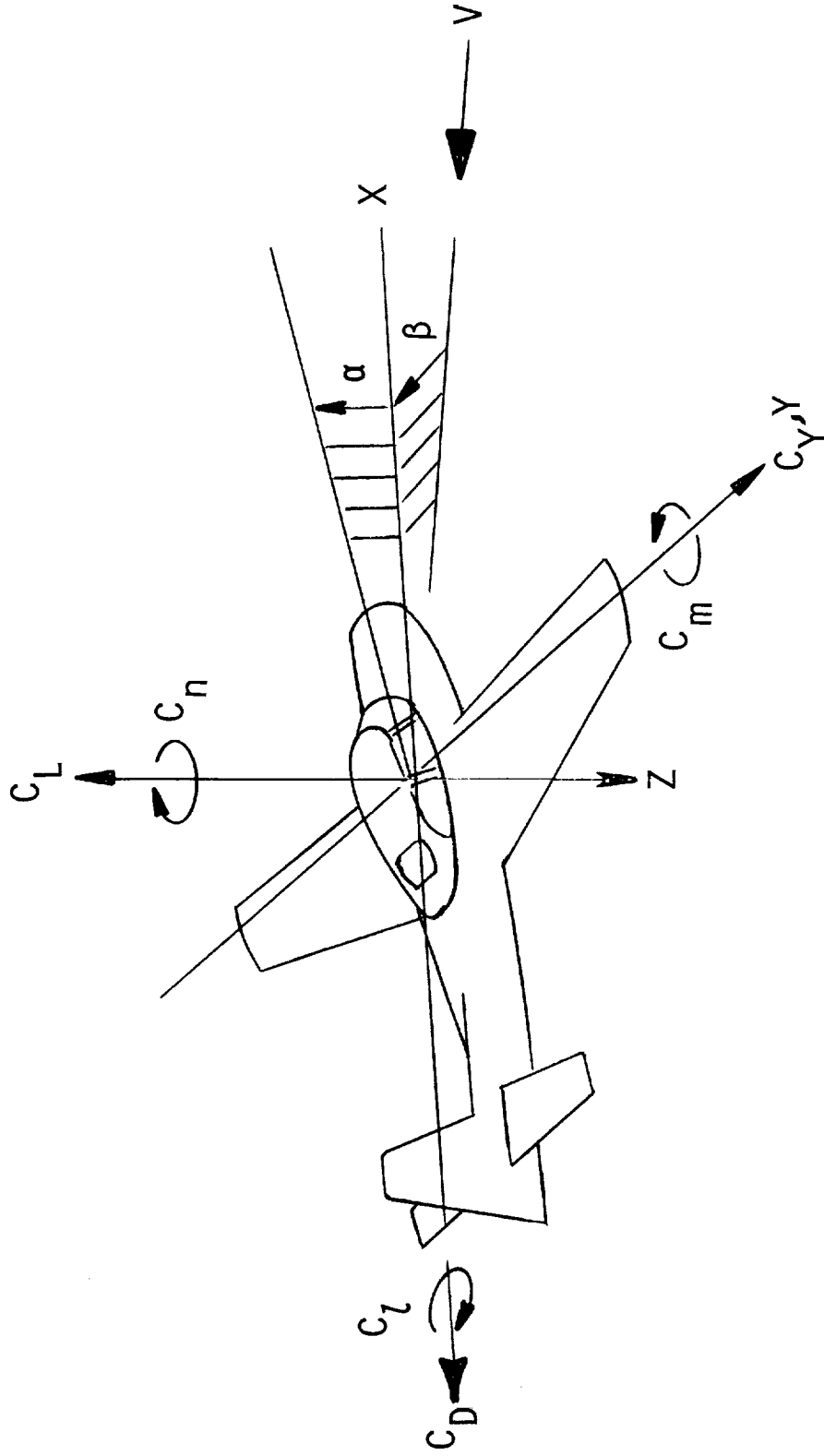


Figure 1.- System of stability axes and positive sense of angles, forces, and moments.

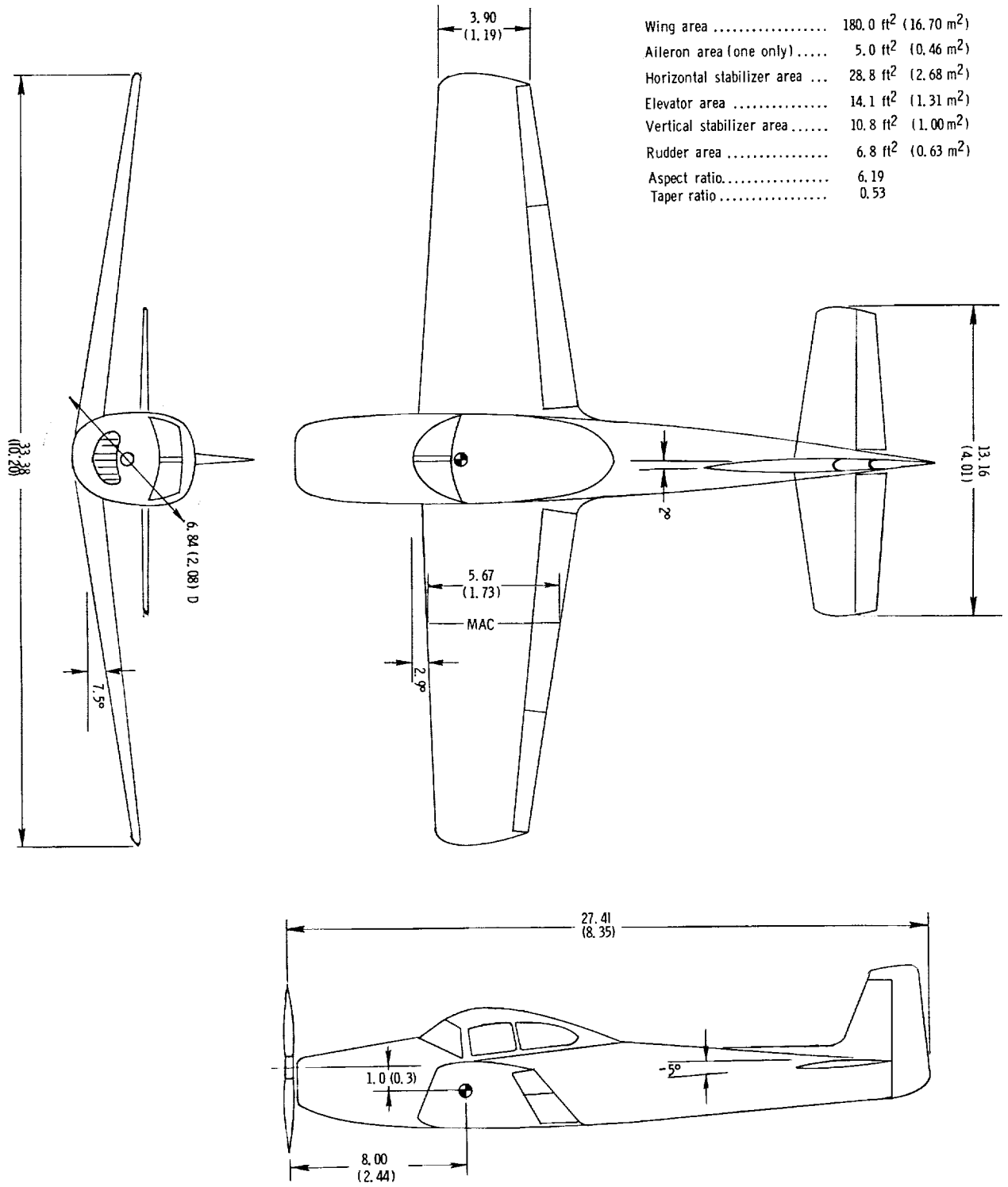


Figure 2.- Three-view drawing and principal dimensions. All dimensions are in feet (meters).  $i_t$  is normally  $0^\circ$  set at  $-5^\circ$  for these tests.



L-69-6944

Figure 3.- Photograph of airplane in Langley full-scale tunnel.

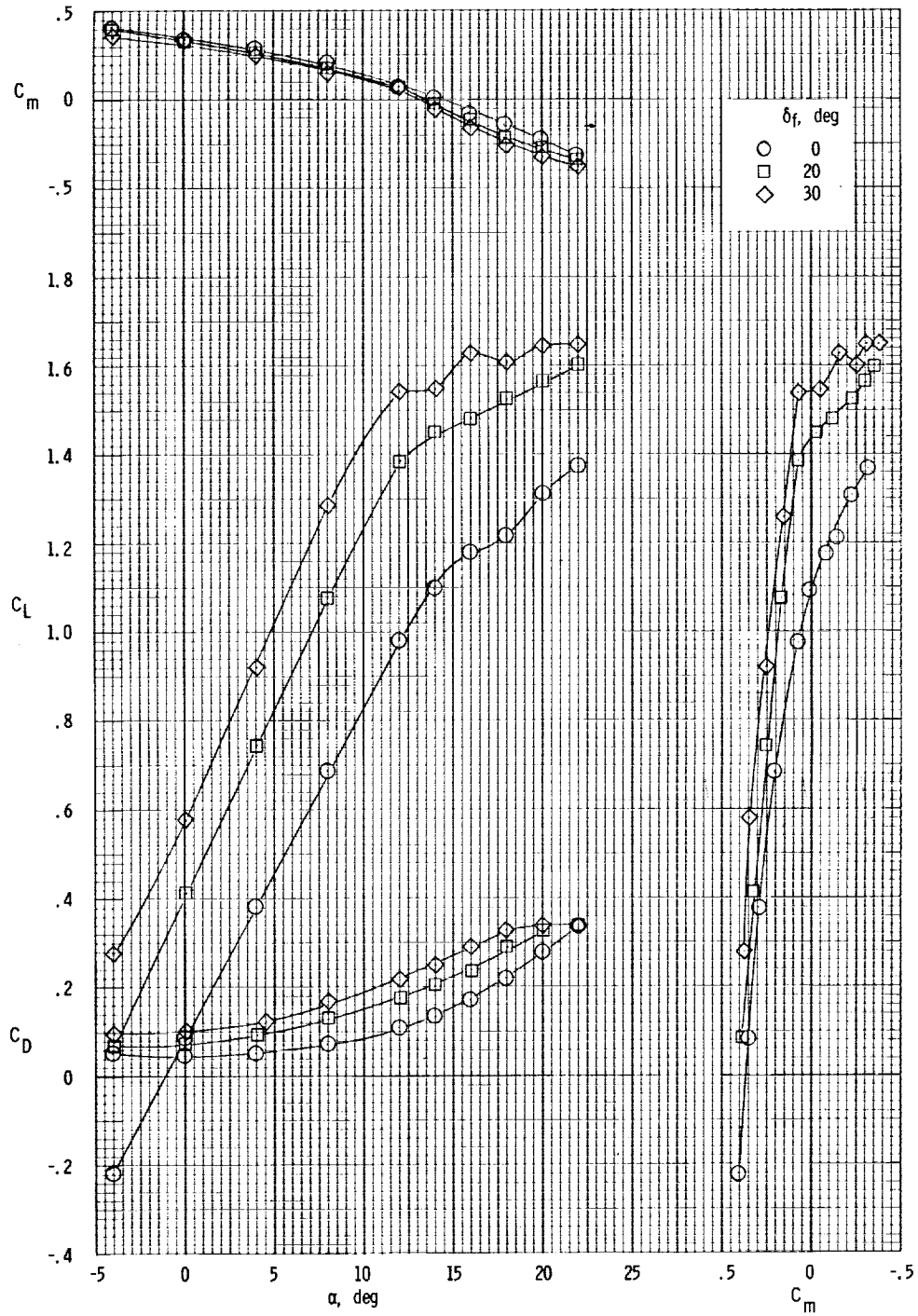
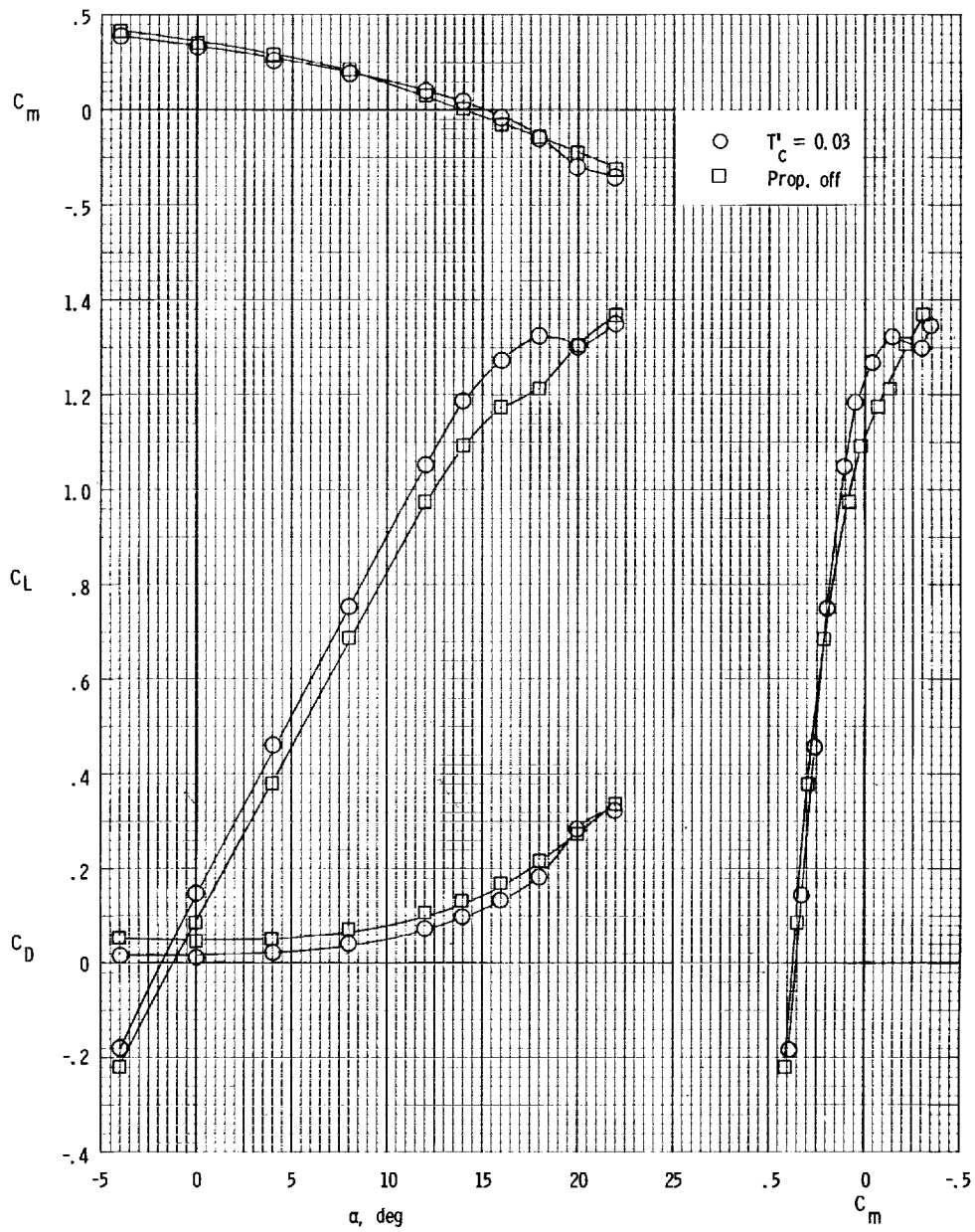
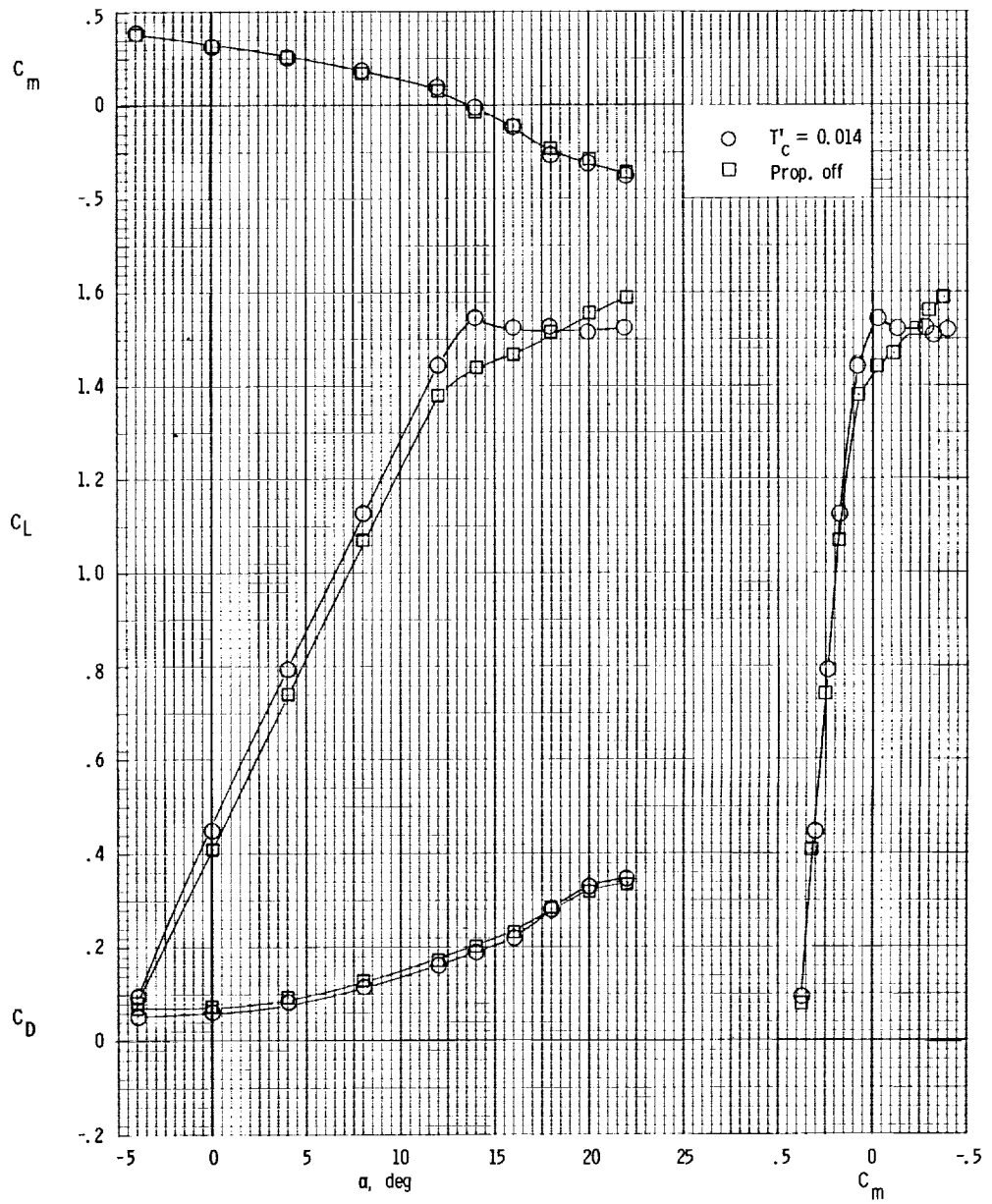


Figure 4.- Longitudinal aerodynamic characteristics of the airplane with propeller removed for several flap deflections.  $i_t = -5^\circ$ .



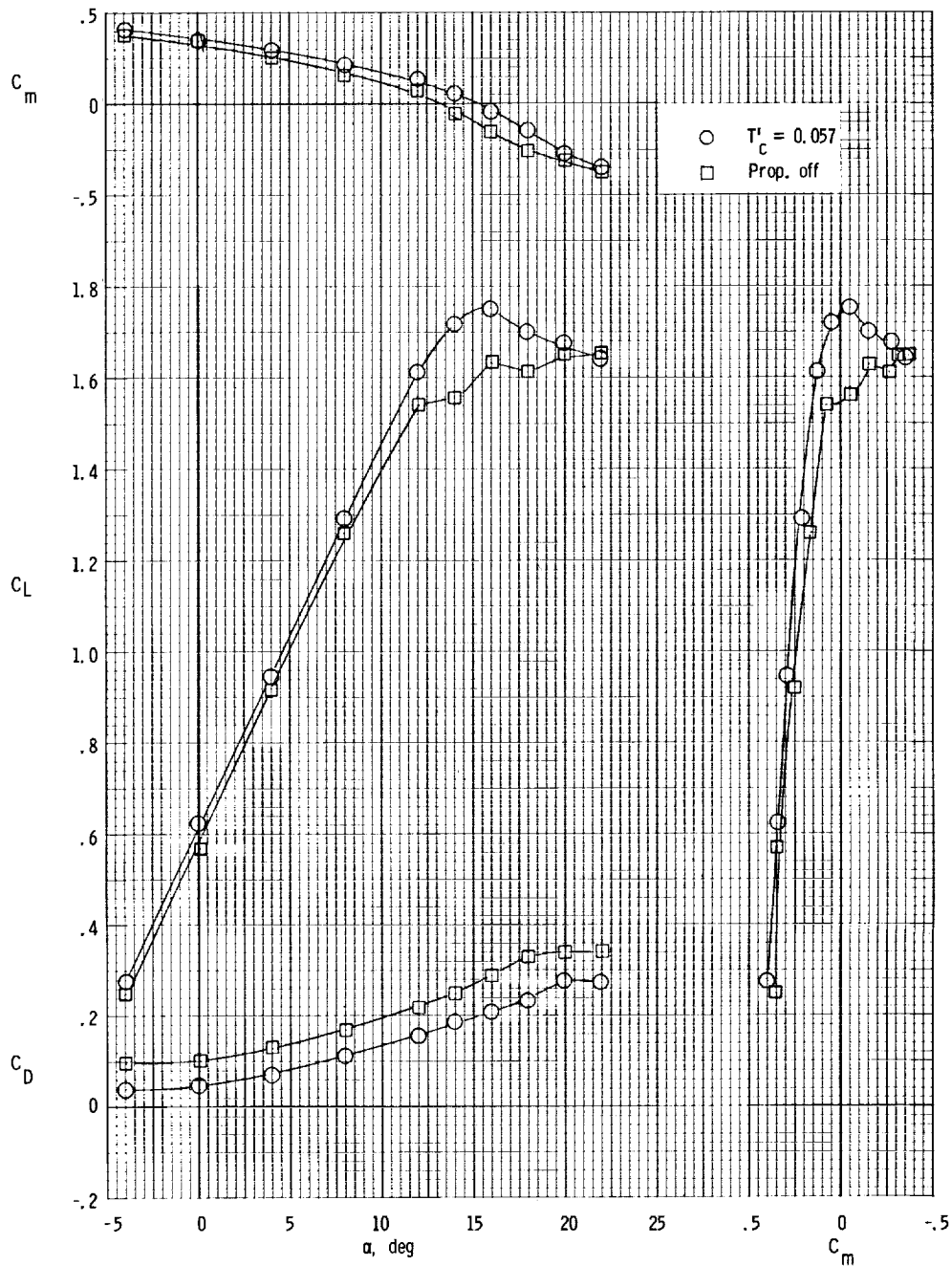
(a)  $\delta_f = 0^\circ$ .

Figure 5.- Longitudinal aerodynamic characteristics with propeller removed and at low power with propeller on for several flap deflections.  $l_t = -5^\circ$ .



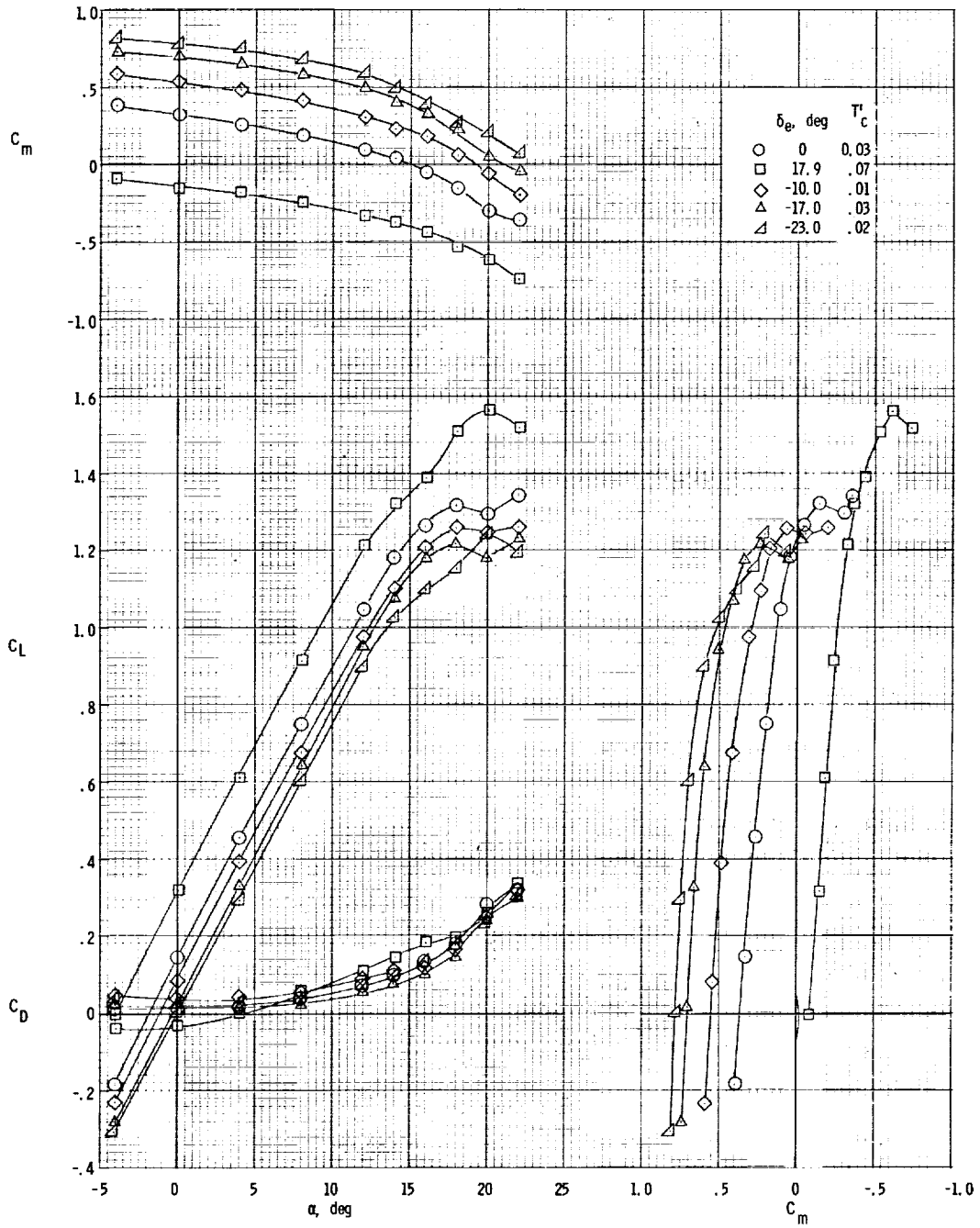
(b)  $\delta_f = 20^\circ$ .

Figure 5.- Continued.



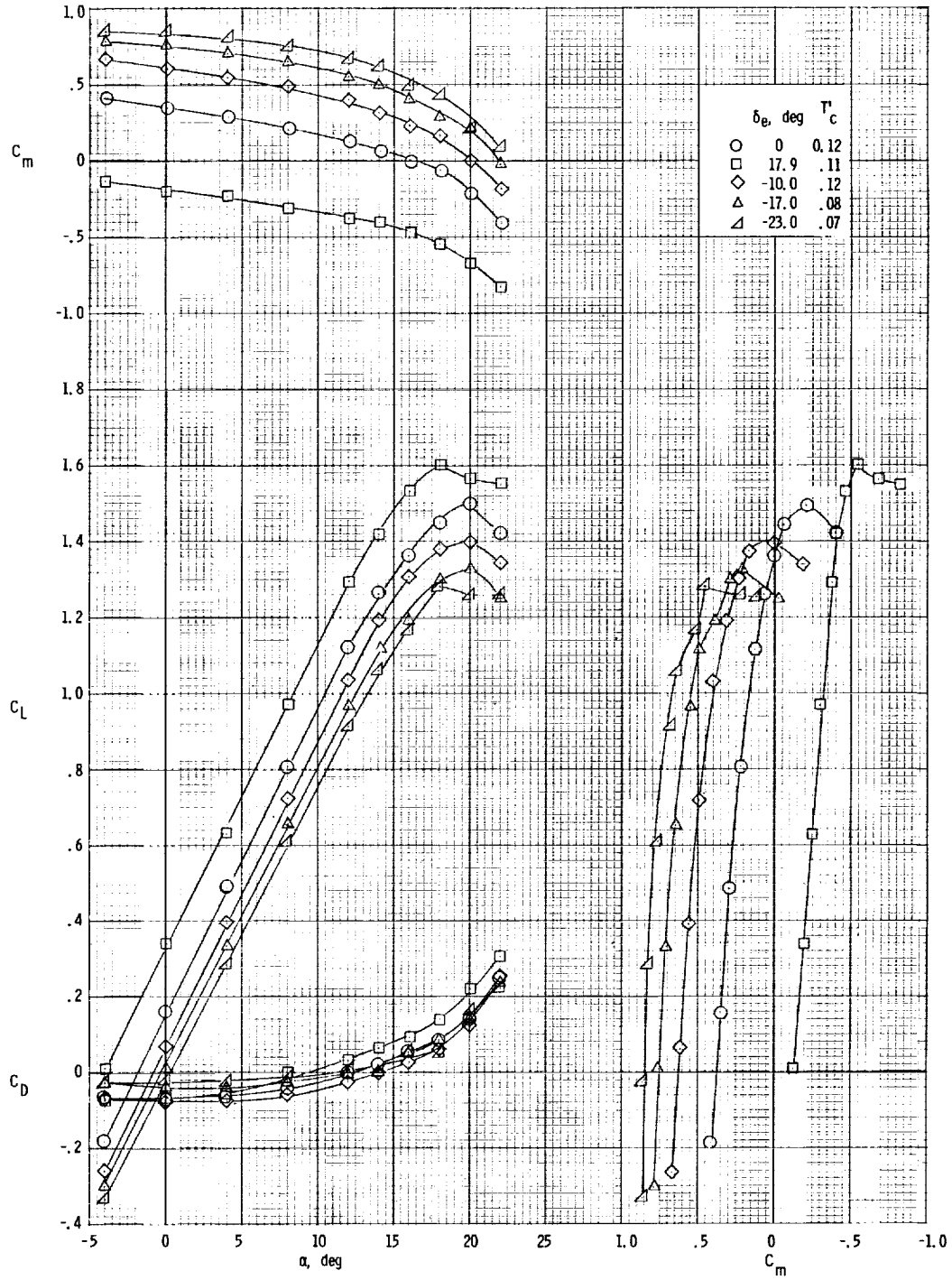
(c)  $\delta_f = 30^\circ$ .

Figure 5.- Concluded.



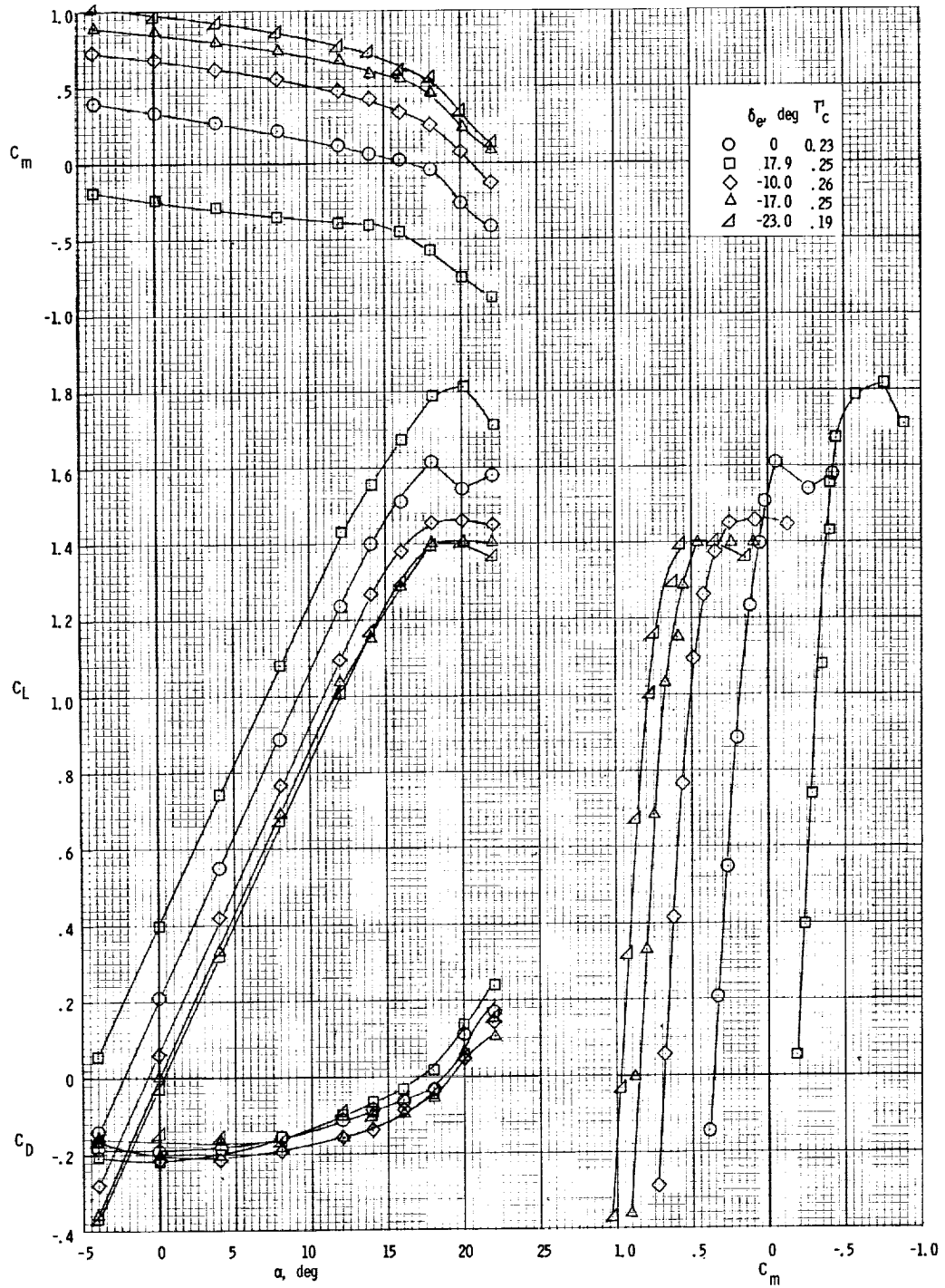
(a)  $T_c' \approx 0.03$ .

Figure 6.- Longitudinal aerodynamic characteristics of the airplane for several thrust coefficients for  $\delta_t = 0^\circ$  and  $i_t = -5^\circ$ .



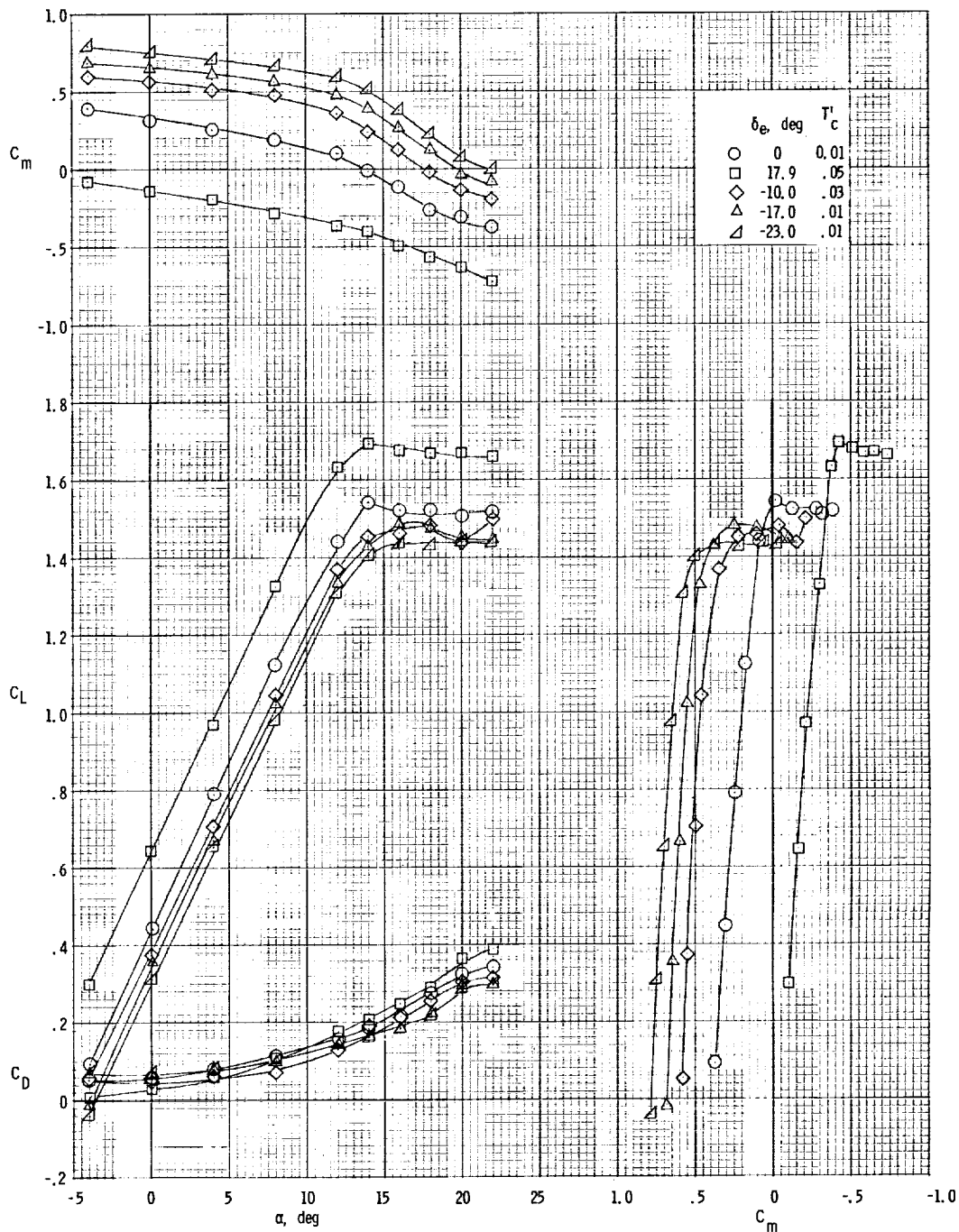
(b)  $T'_c \approx 0.10$ .

Figure 6.- Continued.



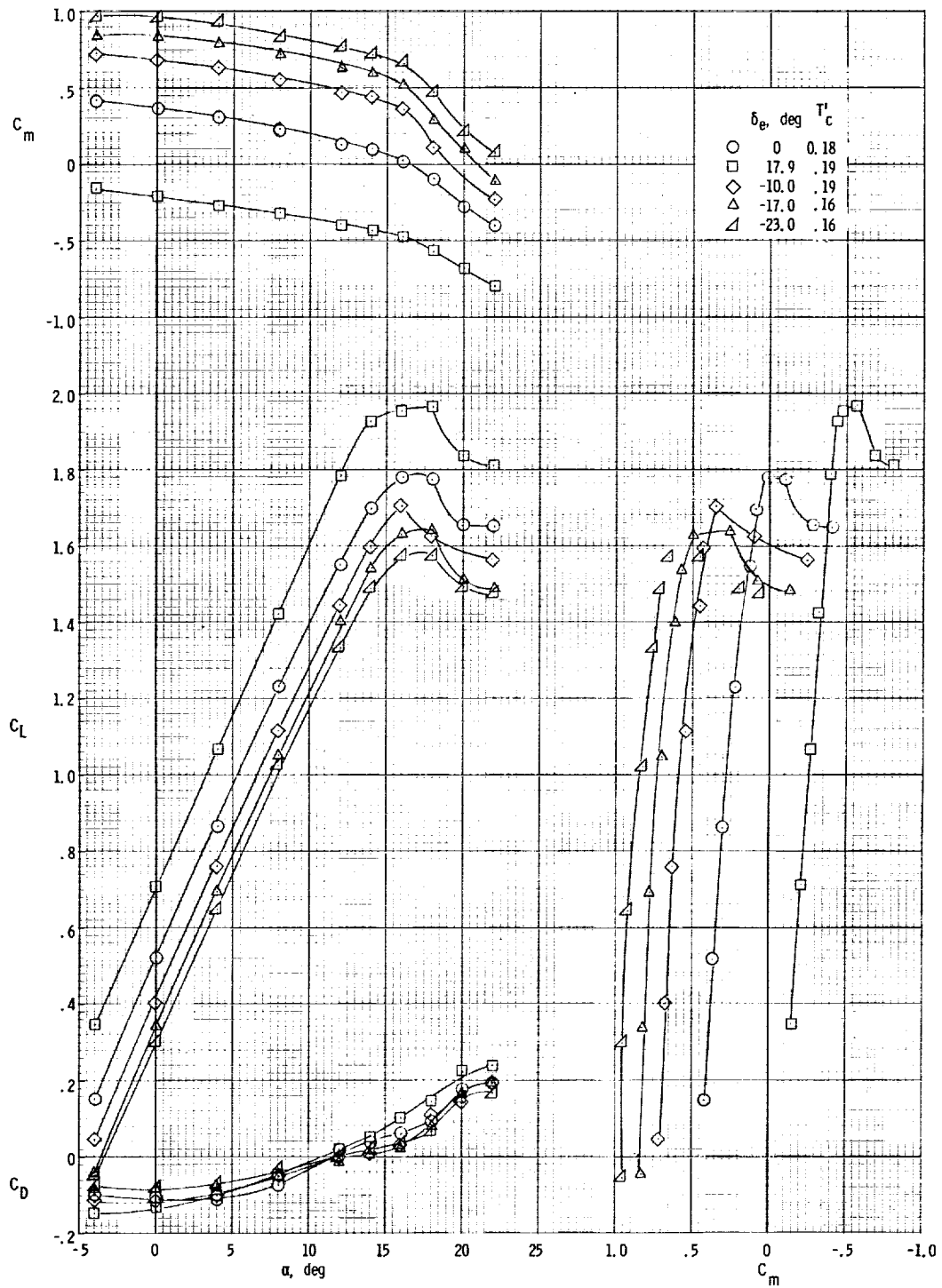
(c)  $T_c^1 \approx 0.23$ .

Figure 6.- Concluded.



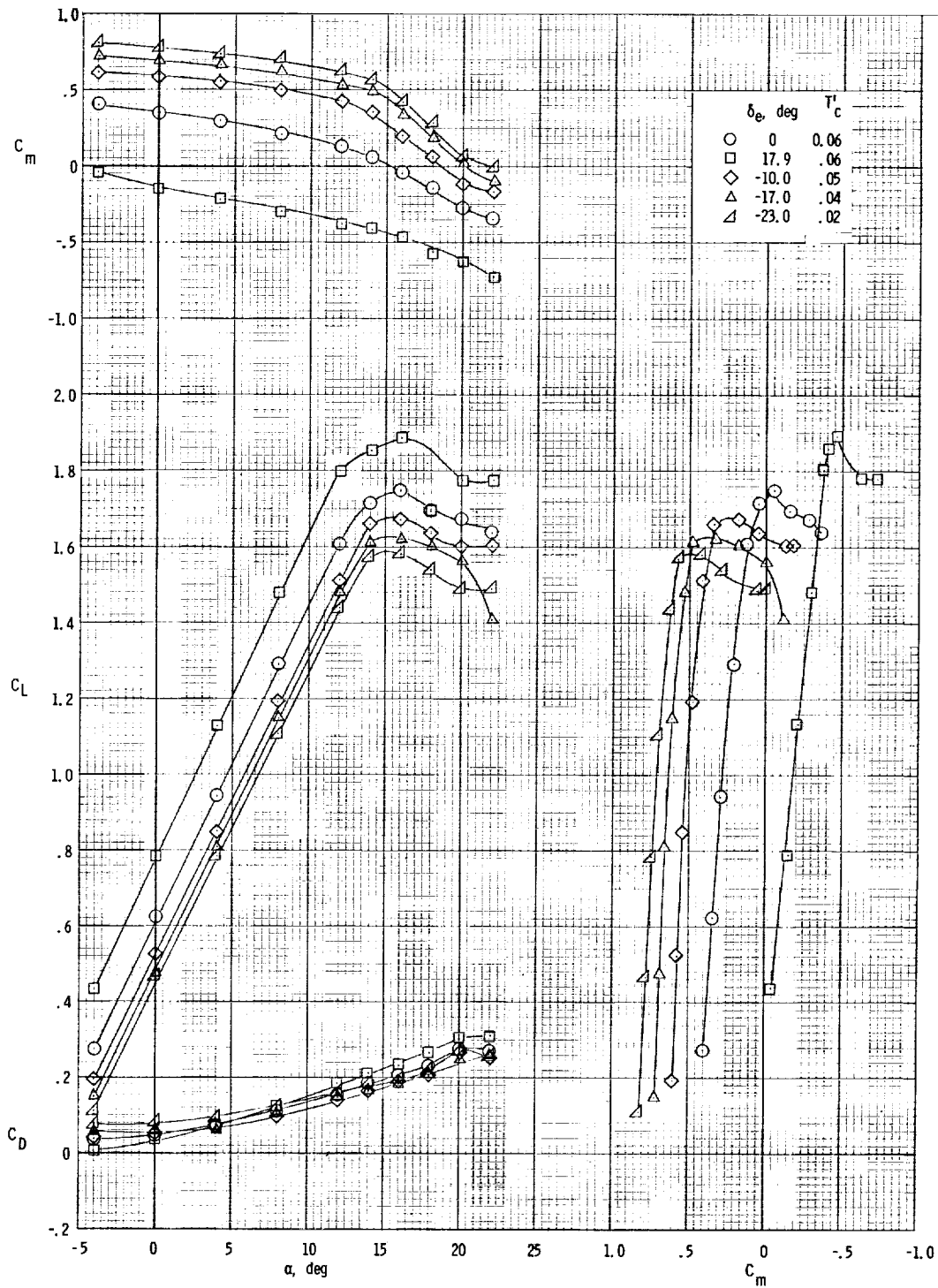
(a)  $T'_c \approx 0.01$ .

Figure 7.- Longitudinal aerodynamic characteristics of the airplane for several thrust coefficients for  $\delta_f = 20^\circ$  and  $i_t = -5^\circ$ .



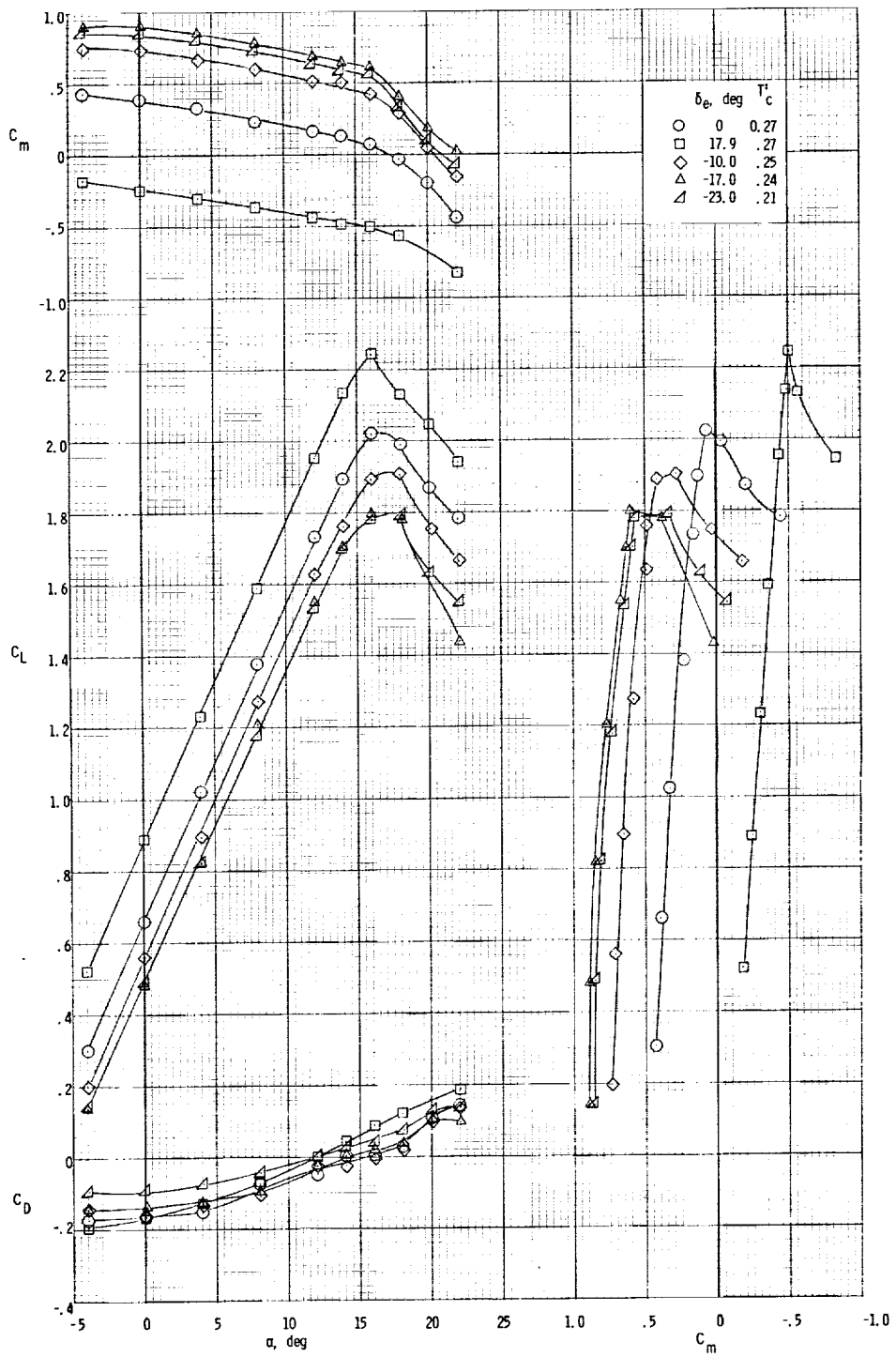
(b)  $T'_c \approx 0.20$ .

Figure 7.- Concluded.



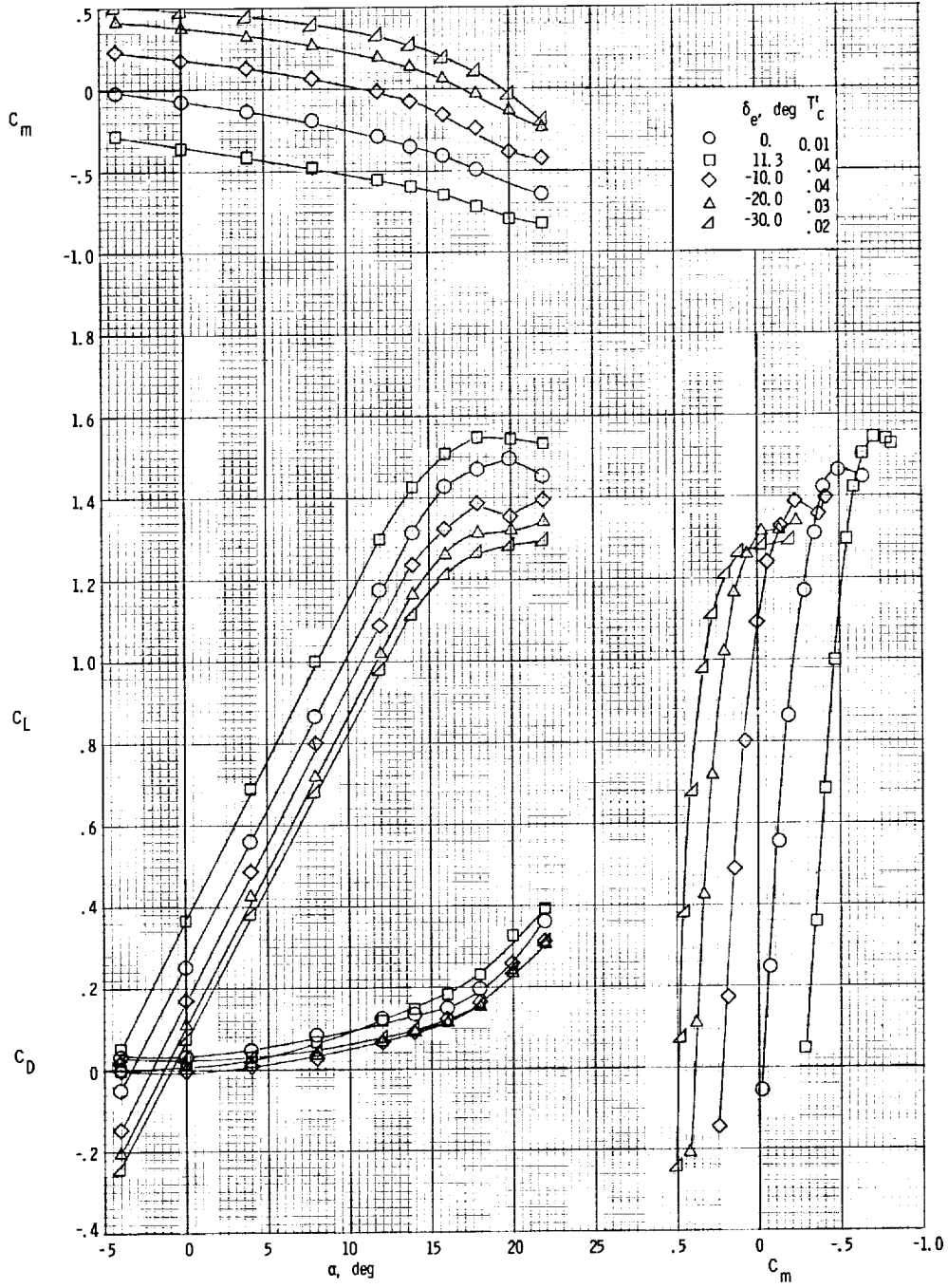
(a)  $T_c' \approx 0.06$ .

Figure 8.- Longitudinal aerodynamic characteristics of the airplane for several thrust coefficients for  $\delta_t = 30^\circ$  and  $i_t = -5^\circ$ .



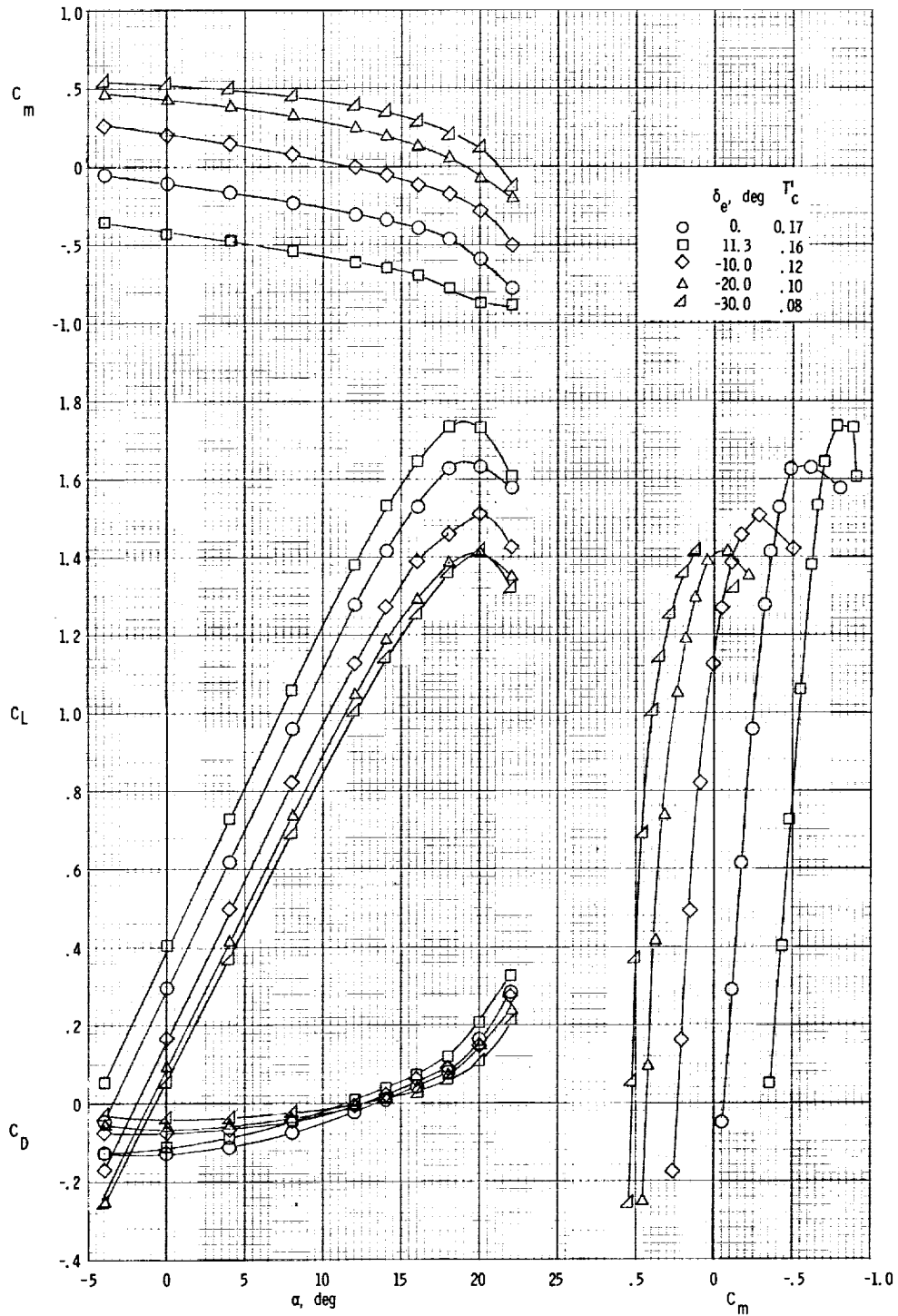
(b)  $T_c \approx 0.25$ .

Figure 8.- Concluded.



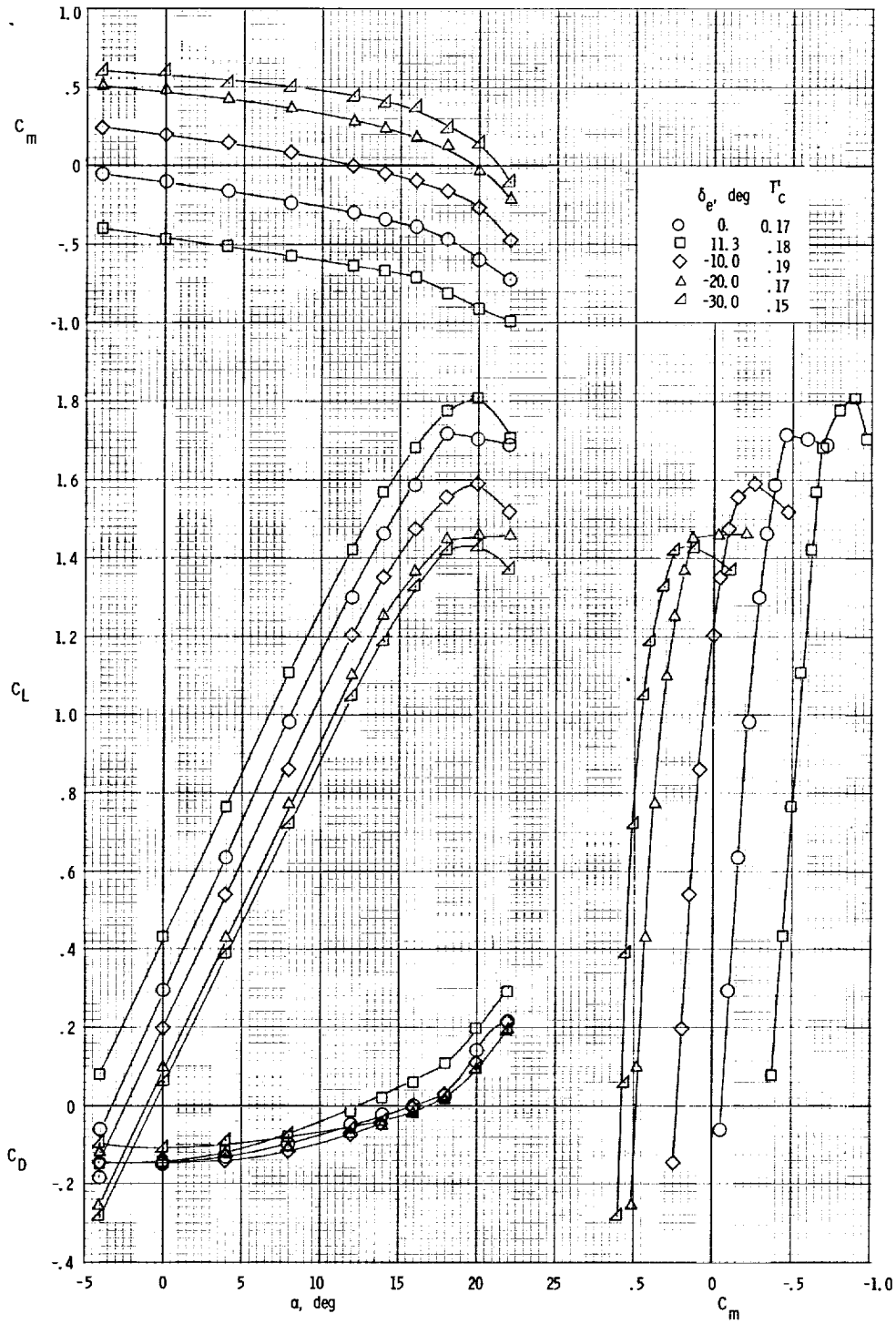
(a)  $T_c' \approx 0.03$ .

Figure 9.- Longitudinal aerodynamic characteristics of the airplane for several thrust coefficients for  $\delta_t = 0^\circ$  and  $i_t = 5^\circ$ .



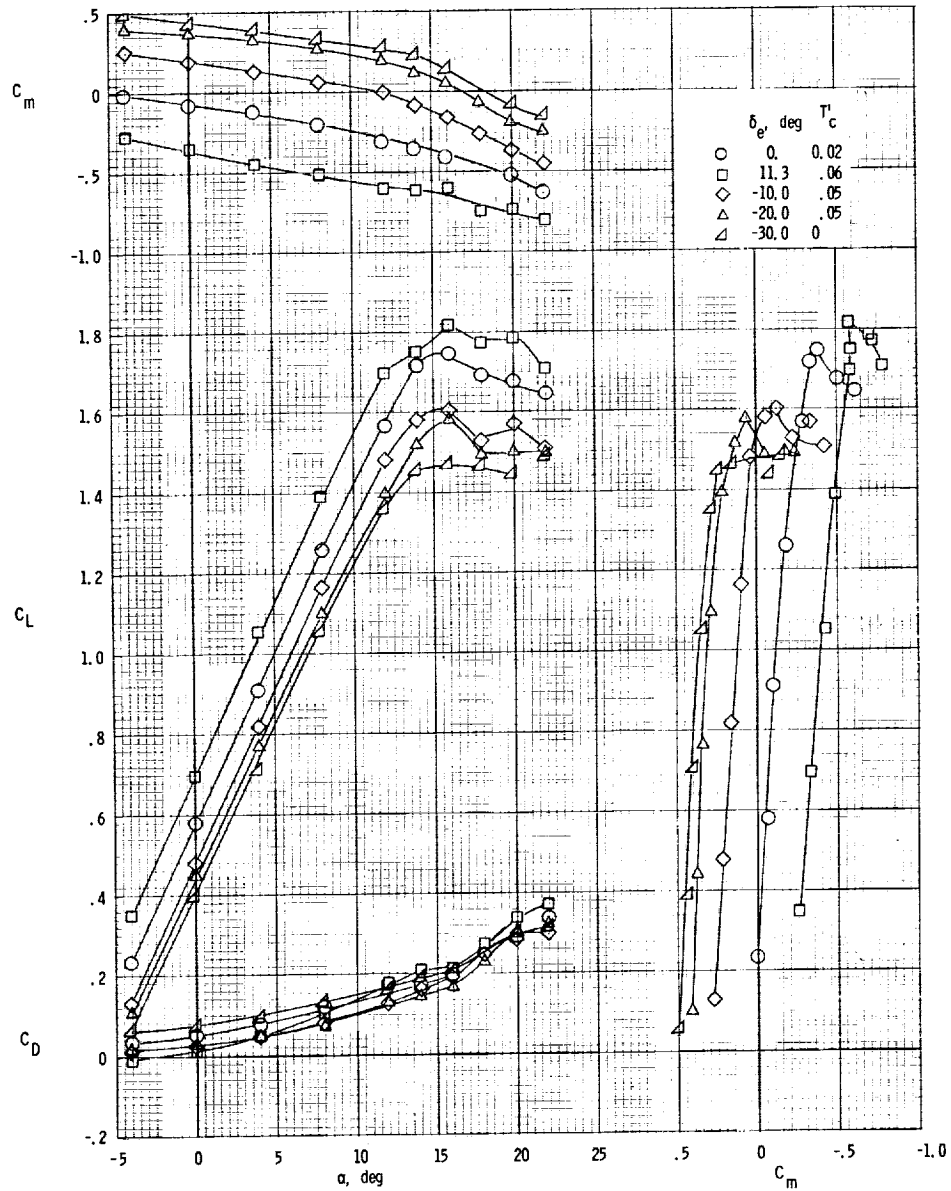
(b)  $T_c' \approx 0.12$ .

Figure 9.- Continued.



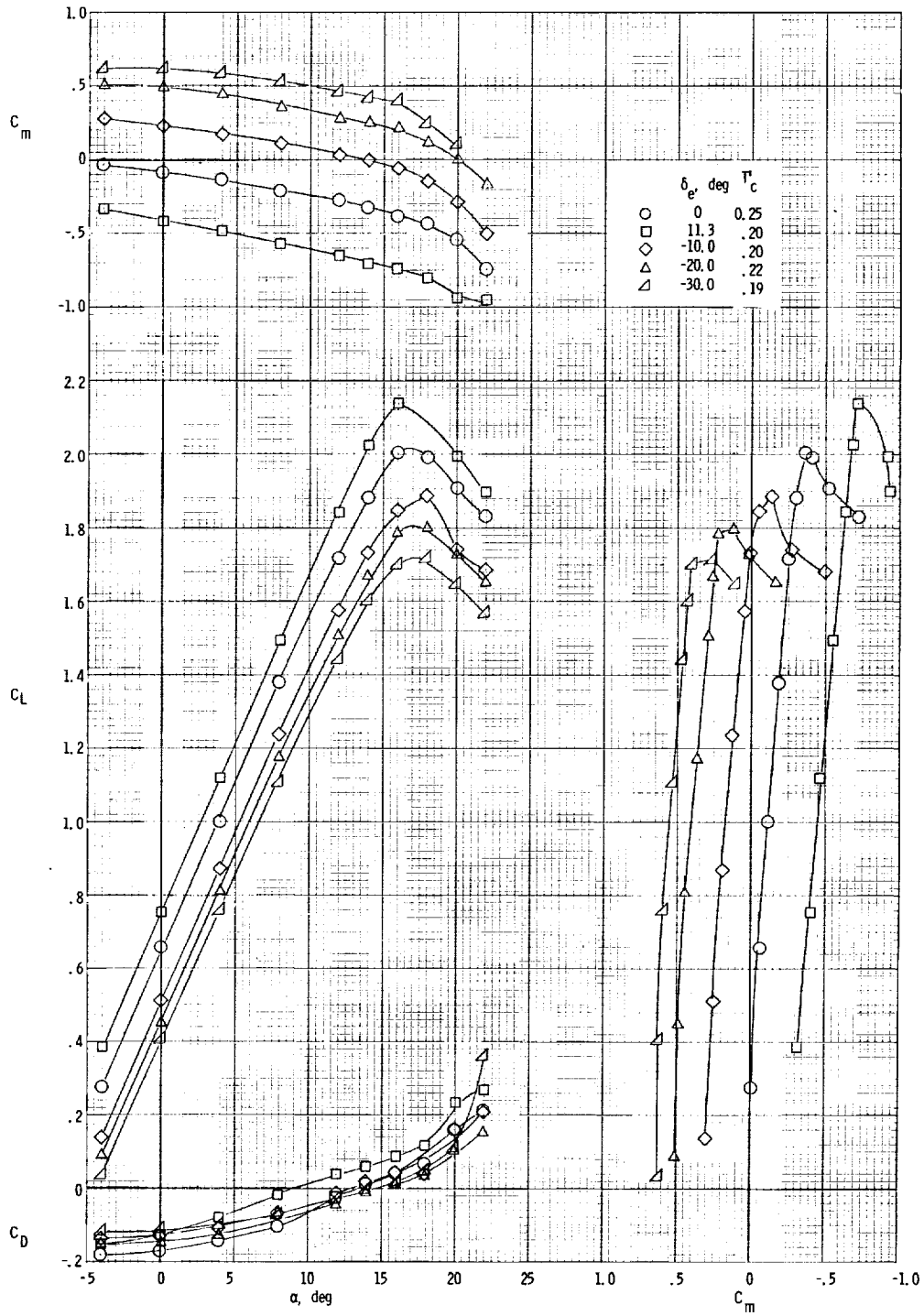
(c)  $T_c \approx 0.17$ .

Figure 9.- Concluded.



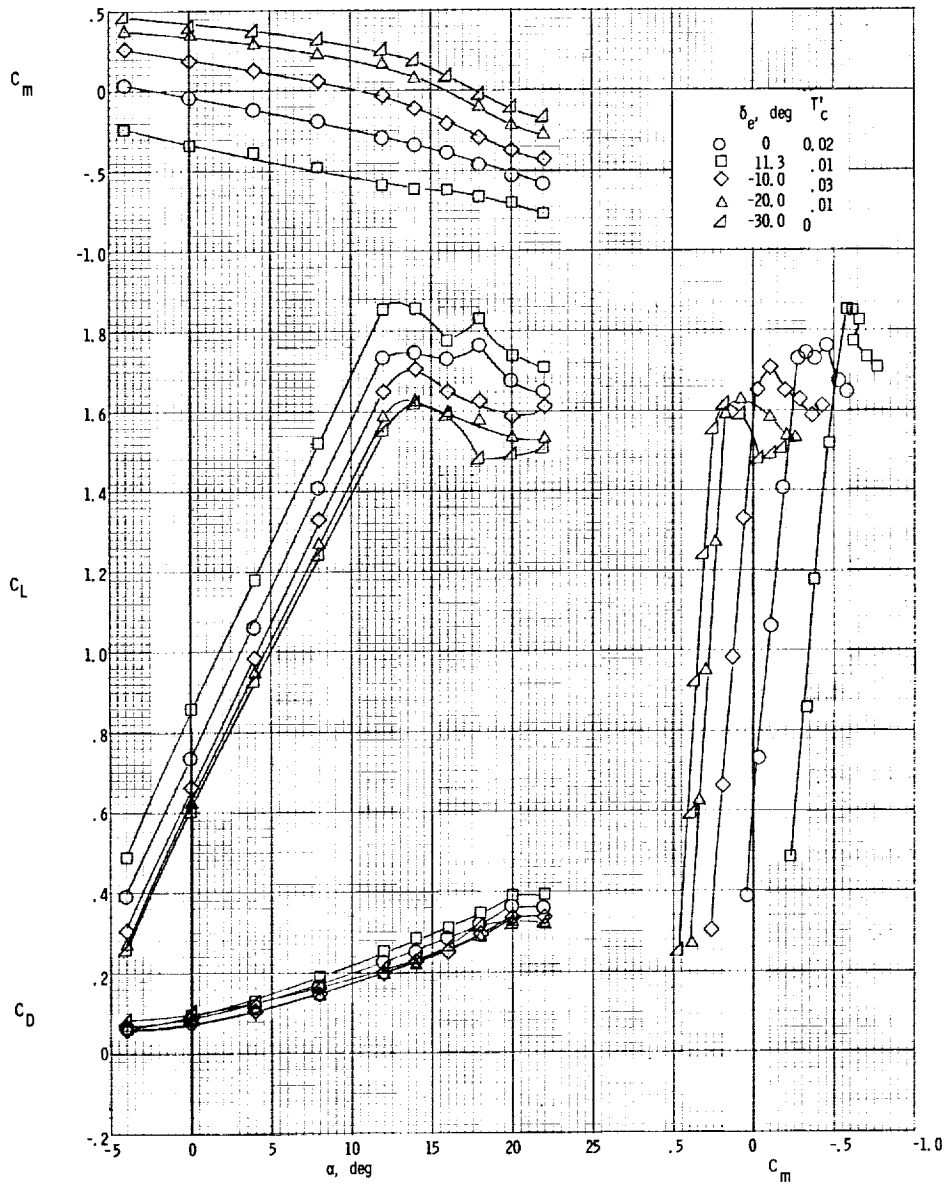
(a)  $T_c \approx 0.03$ .

Figure 10.- Longitudinal aerodynamic characteristics of the airplane for several thrust coefficients for  $\delta_t = 20^\circ$  and  $i_t = 5^\circ$ .



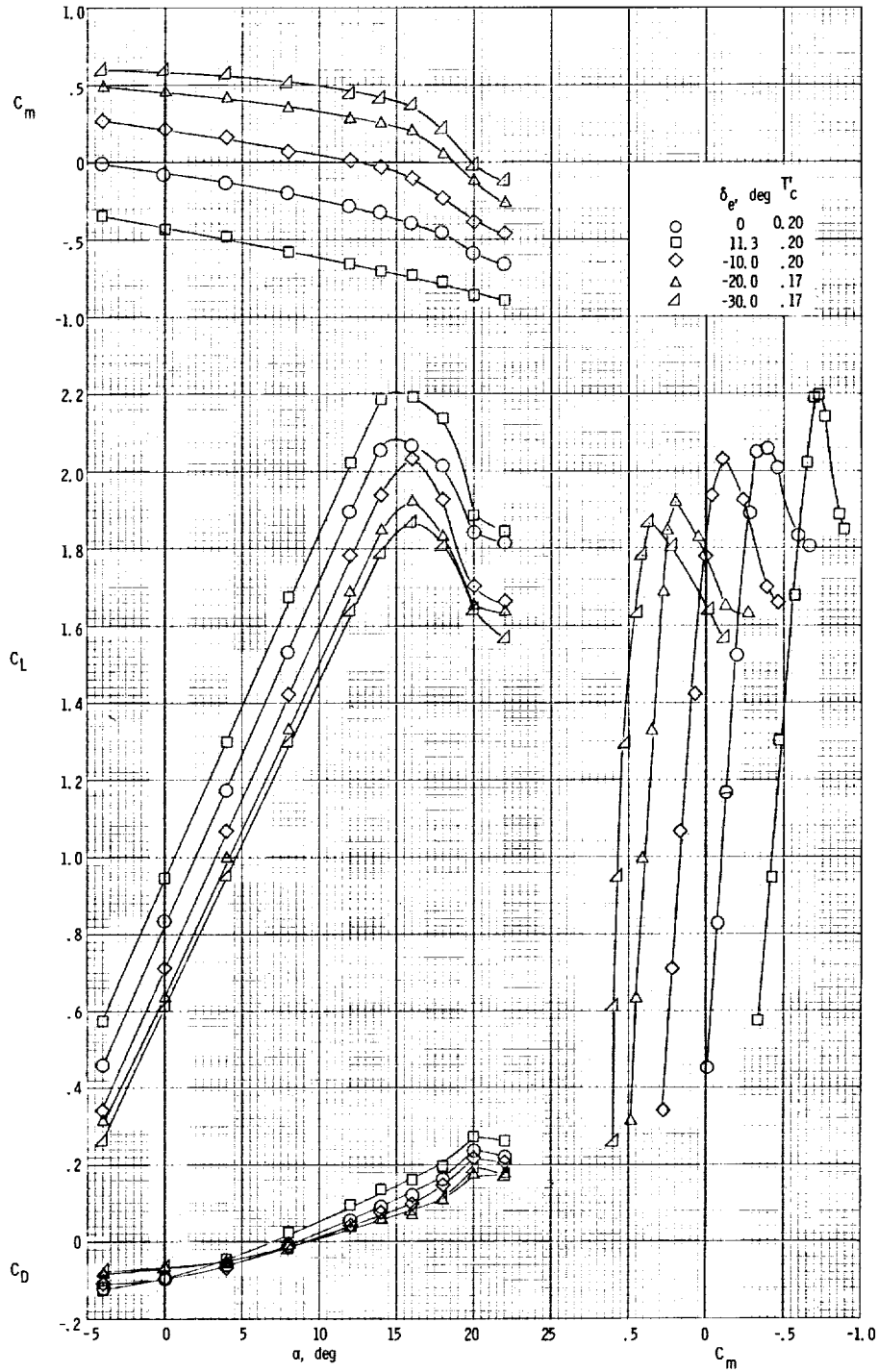
(b)  $T_c' \approx 0.21$ .

Figure 10.- Concluded.



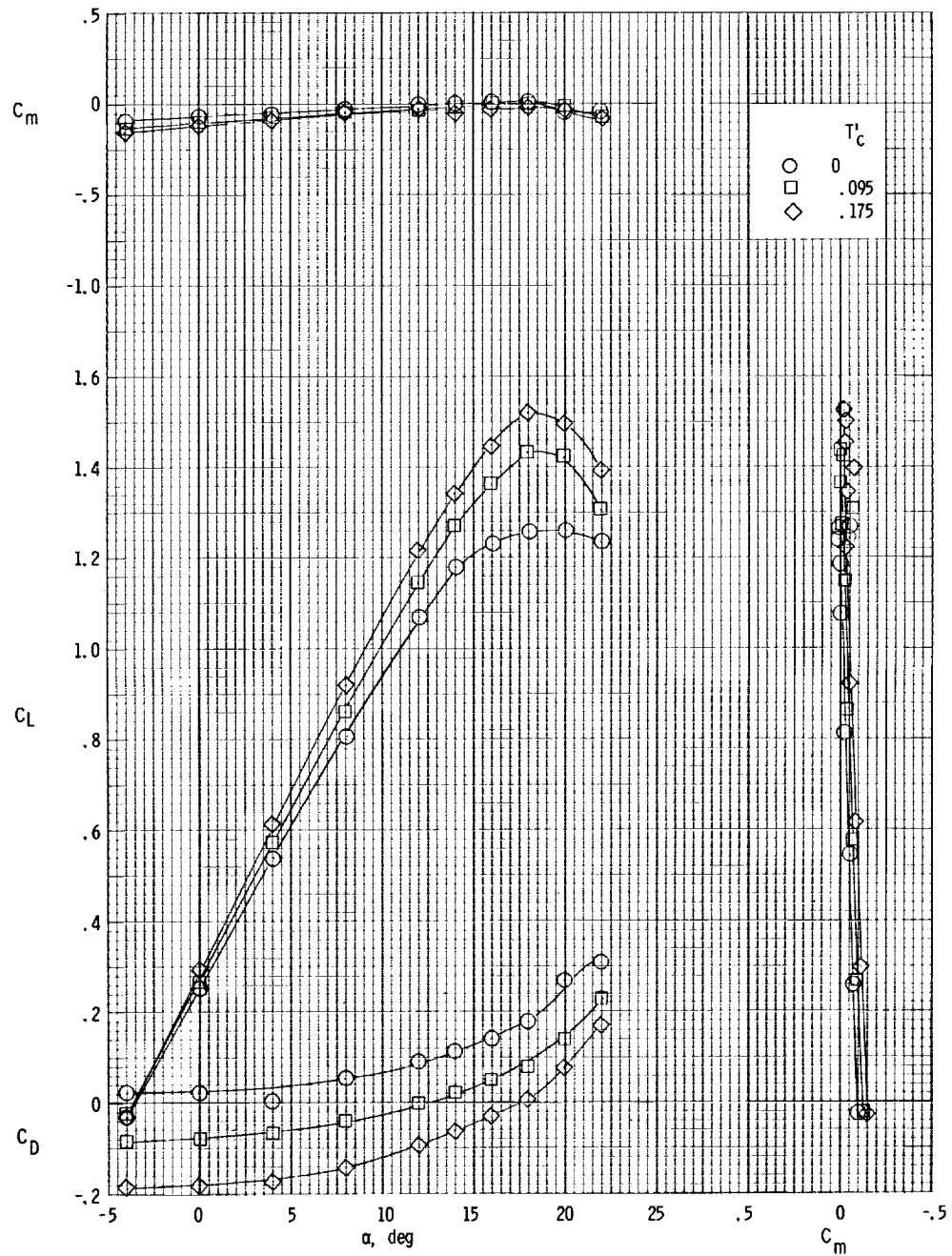
(a)  $T_c \approx 0.01$ .

Figure 11.- Longitudinal aerodynamic characteristics of the airplane for several thrust coefficients for  $\delta_f = 30^\circ$  and  $i_t = 5^\circ$ .



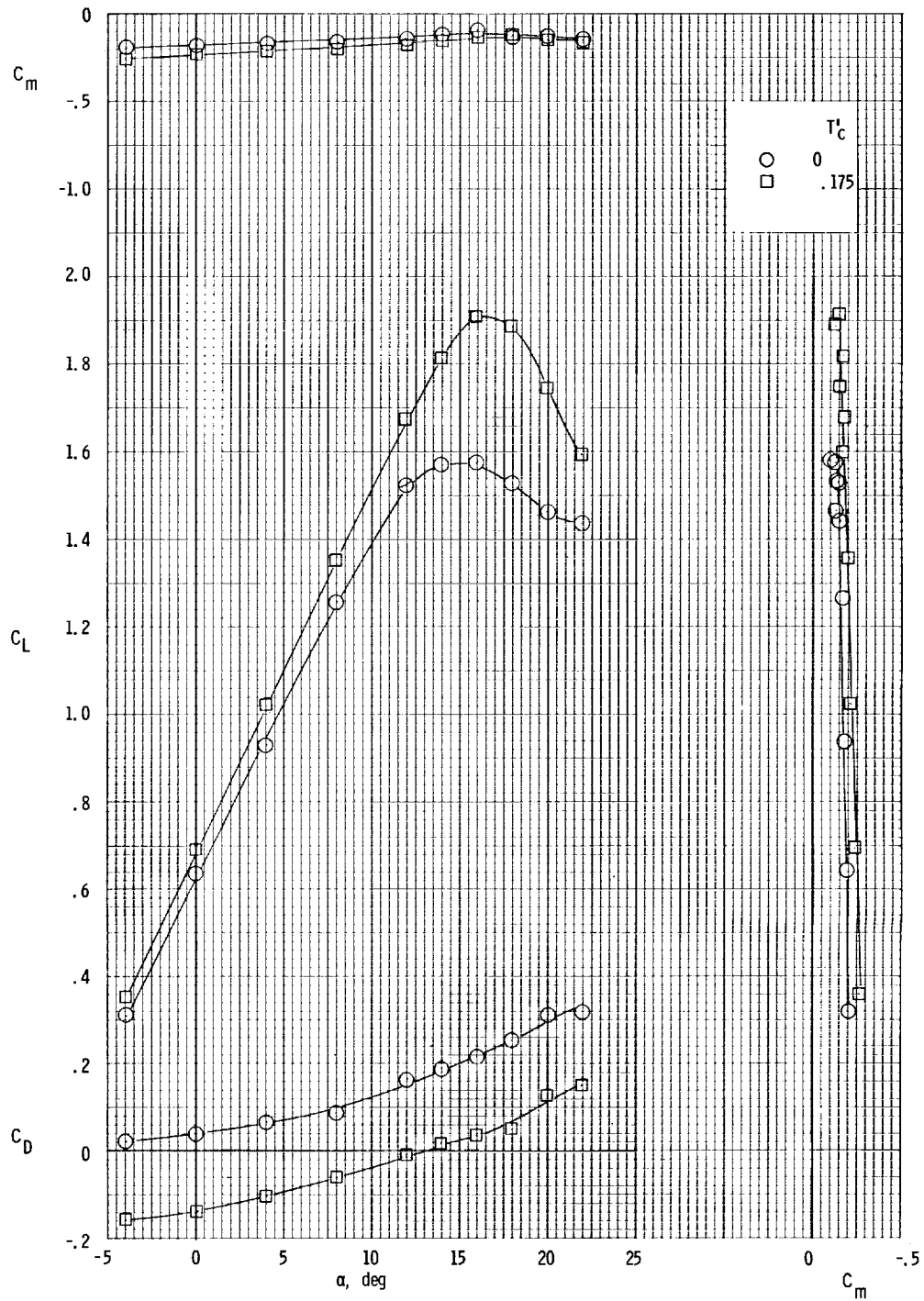
(b)  $T'_c \approx 0.18$ .

Figure 11.- Concluded.



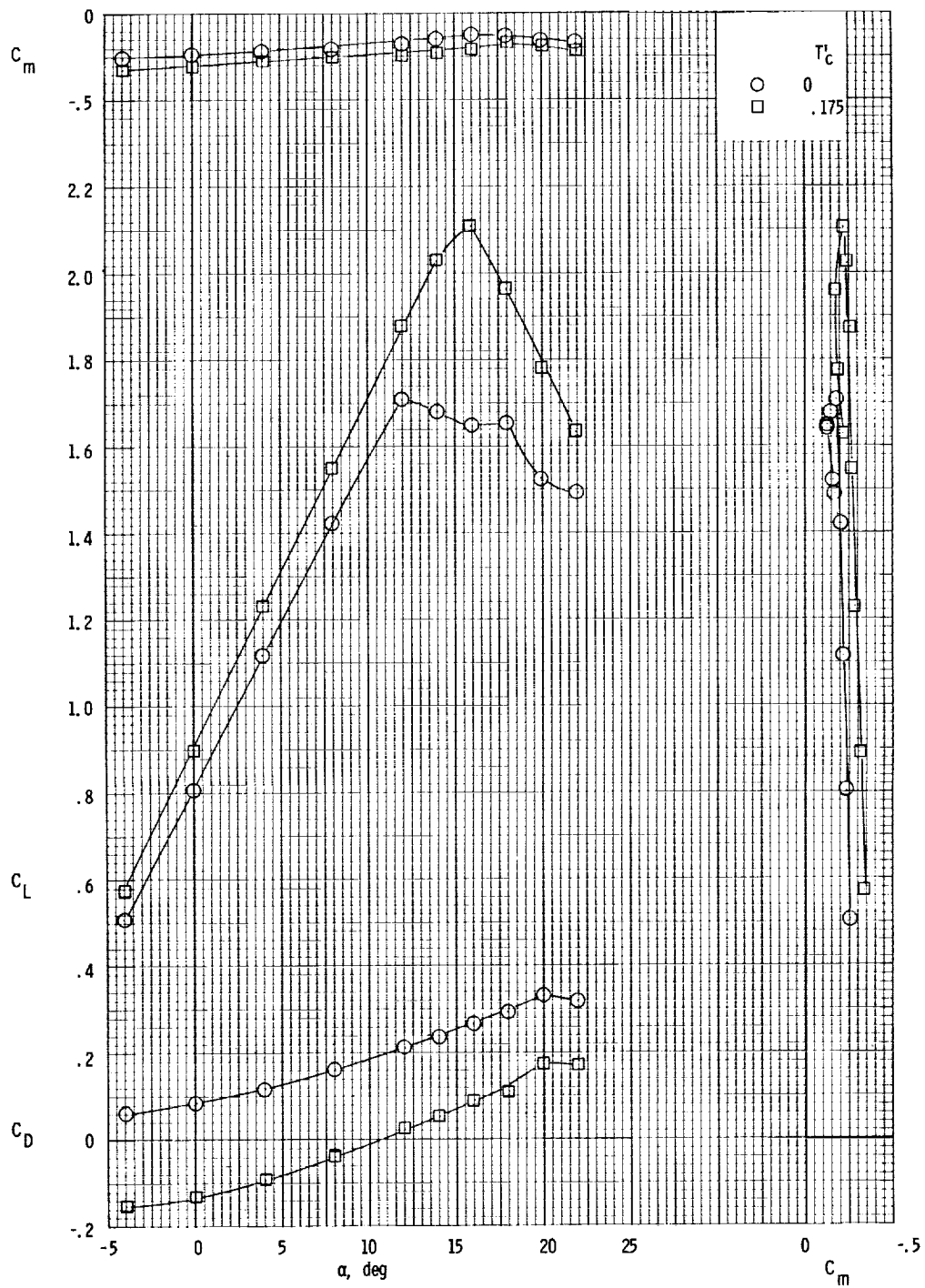
(a)  $\delta_f = 0^\circ$ .

Figure 12.- Longitudinal aerodynamic characteristics of the airplane with the horizontal tail removed for several thrust coefficients and flap deflections.



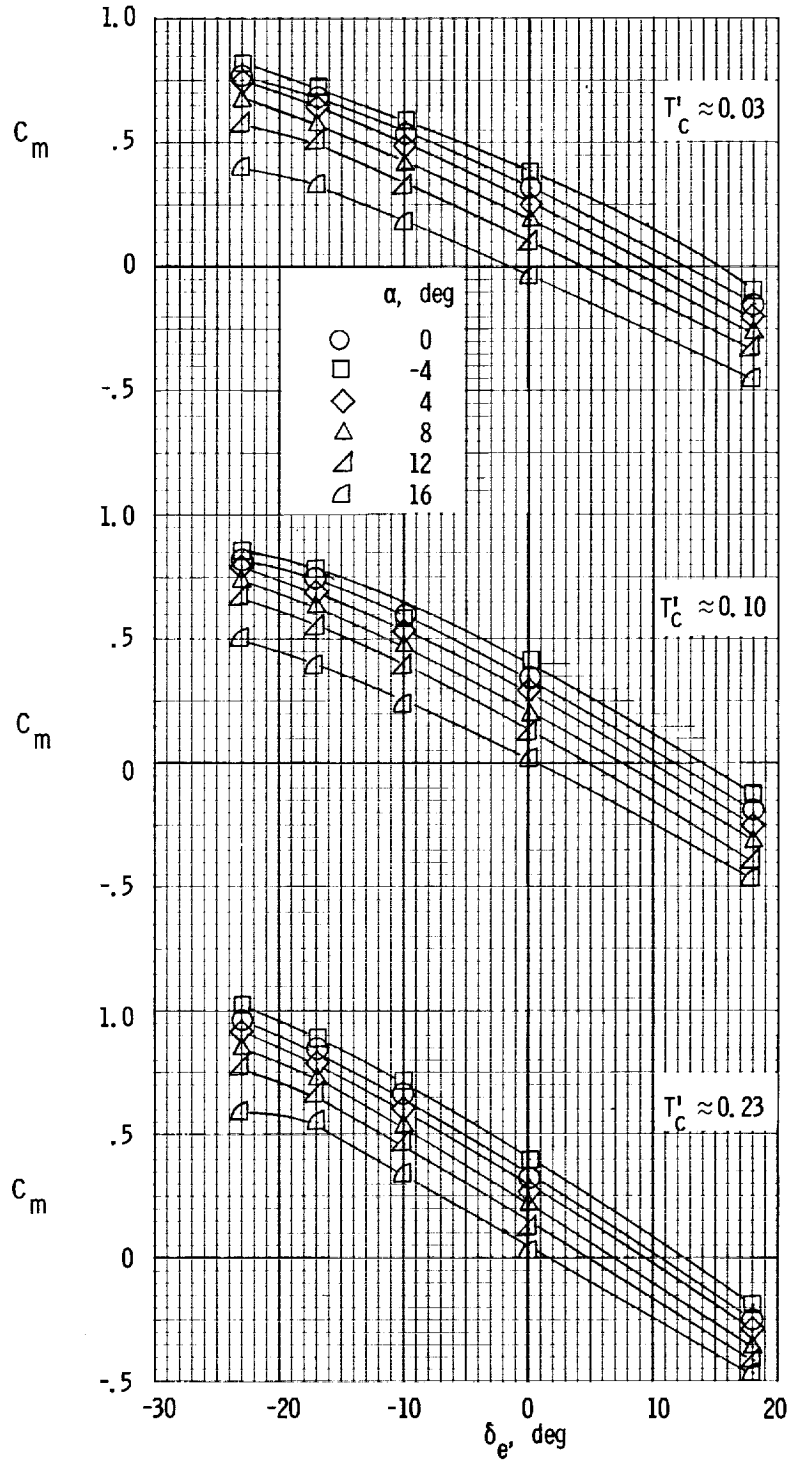
(b)  $\delta_f = 20^\circ$ .

Figure 12.- Continued.



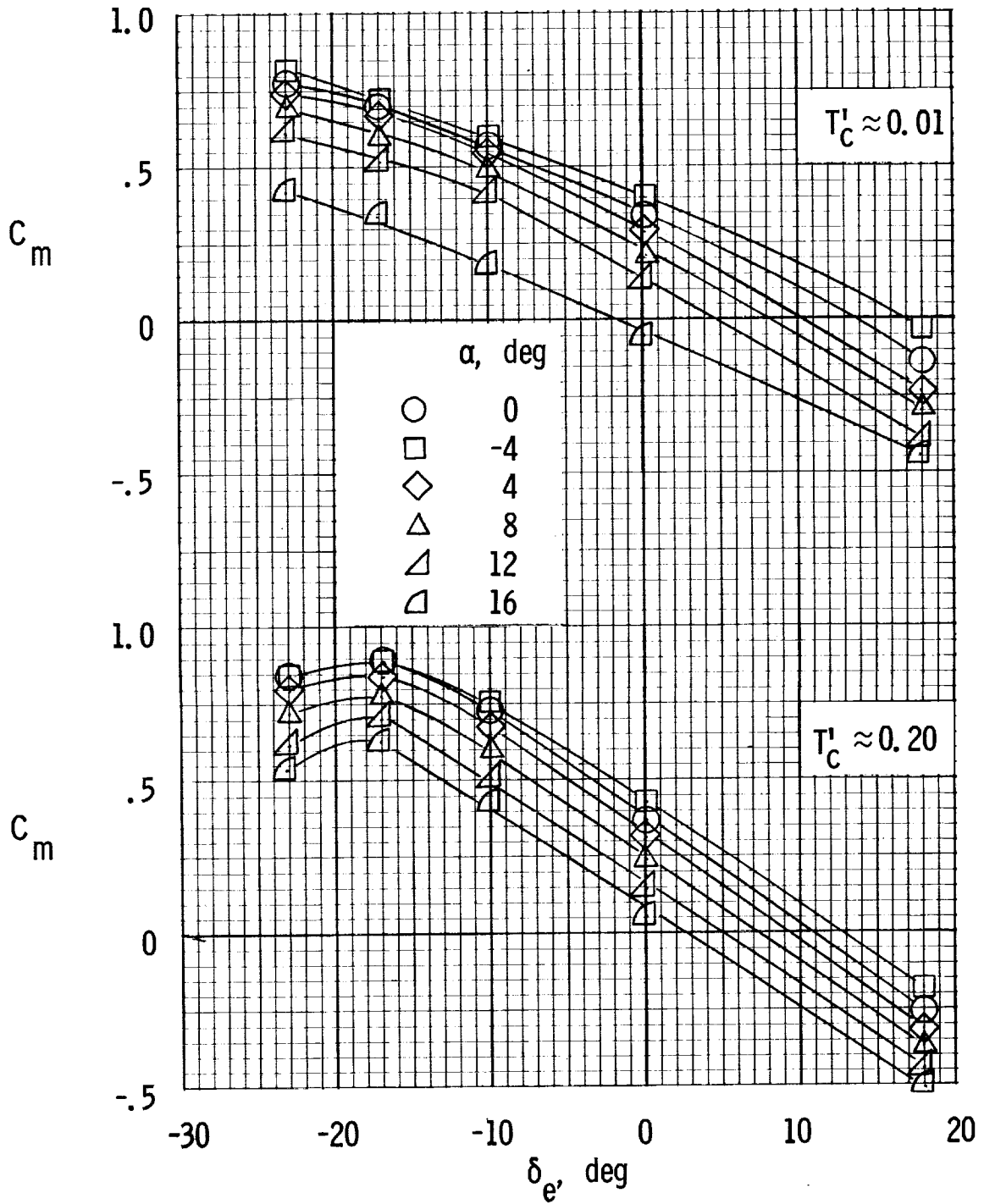
(c)  $\delta_f = 30^\circ$ .

Figure 12.- Concluded.



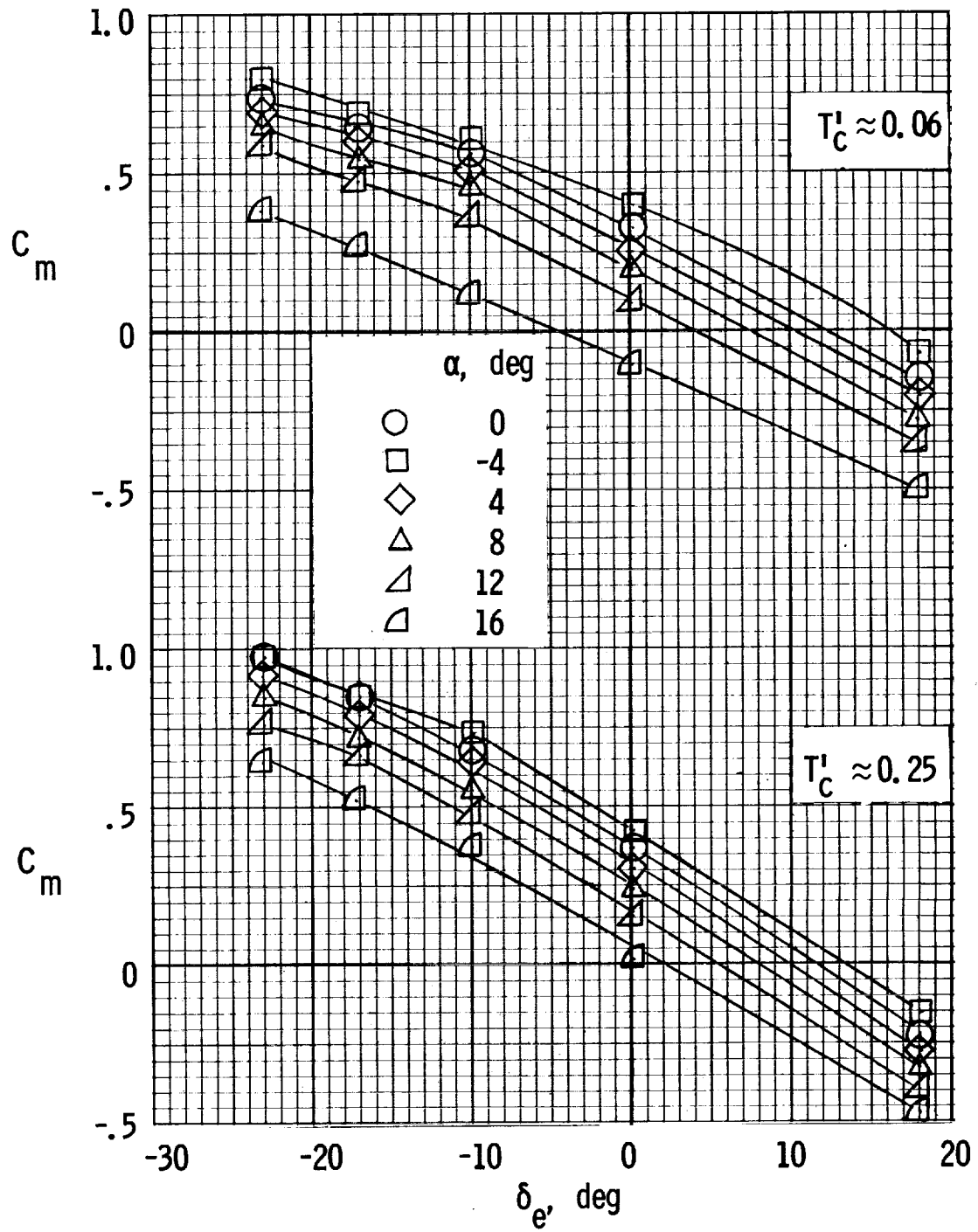
(a)  $\delta_f = 0^\circ$ .

Figure 13.- Variations of pitching-moment coefficient with elevator deflection for several thrust coefficients and flap deflections for  $i_t = -5^\circ$ .



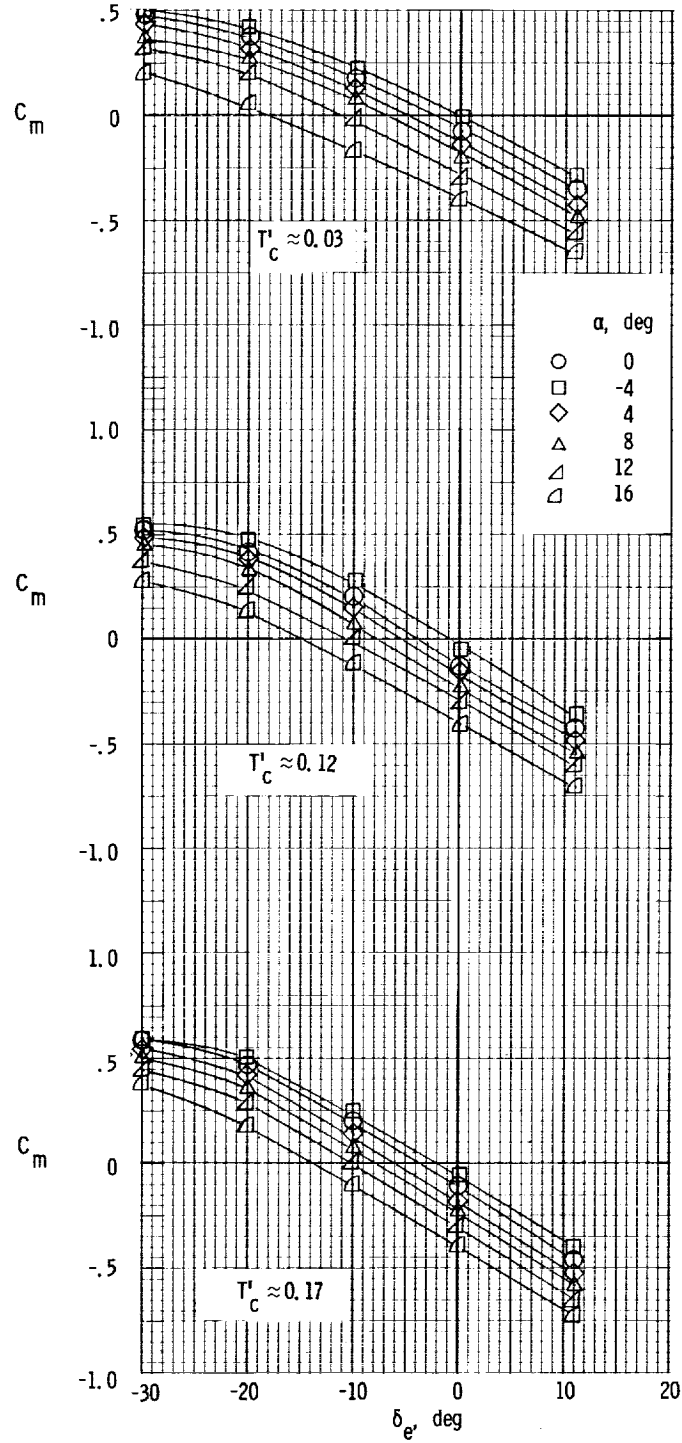
(b)  $\delta_f = 20^\circ$ .

Figure 13.- Continued.



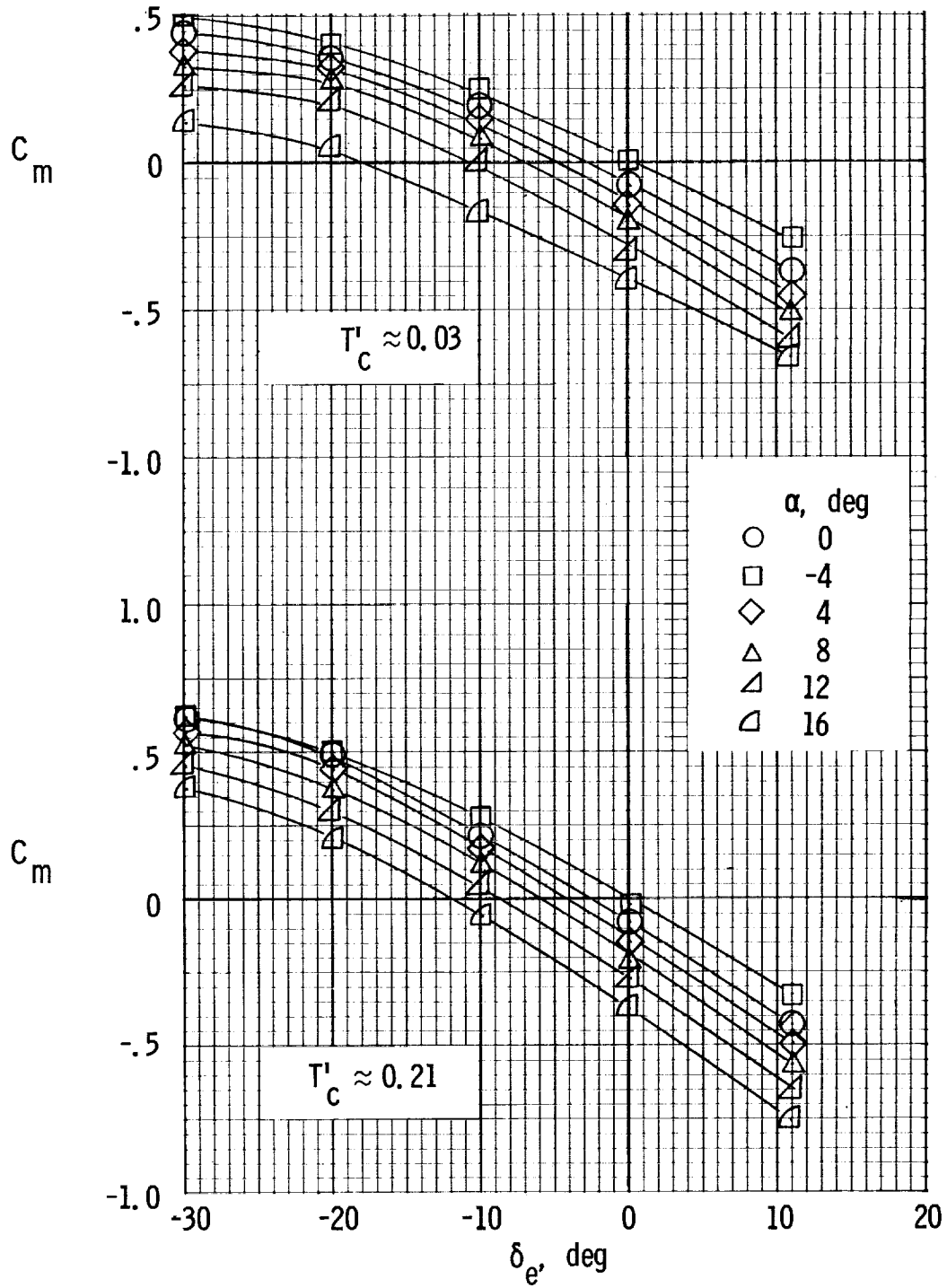
(c)  $\delta_f = 30^\circ$ .

Figure 13.- Concluded.



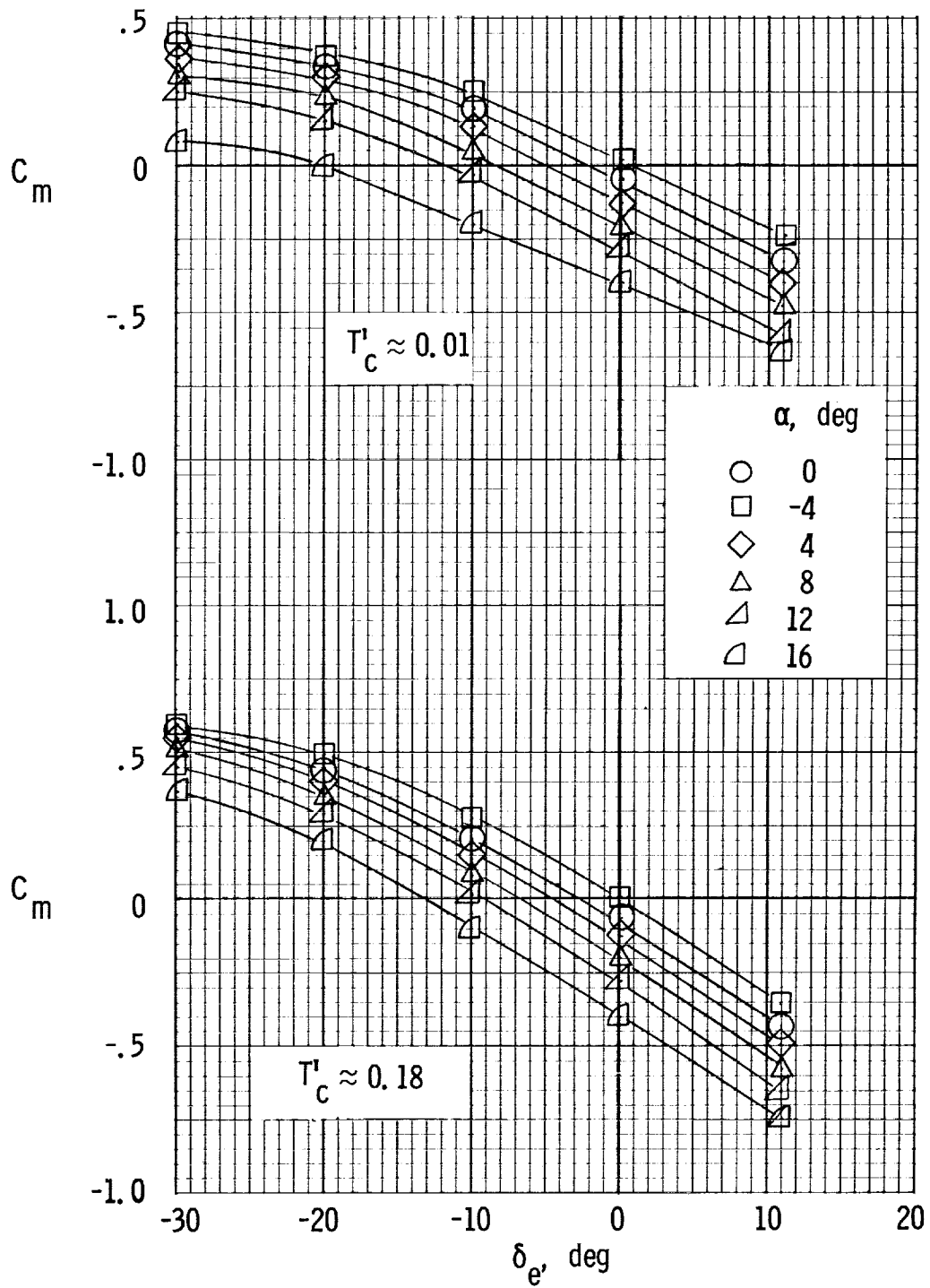
(a)  $\delta_f = 0^\circ$ .

Figure 14.- Variations of pitching-moment coefficient with elevator deflection for several thrust coefficients and flap deflections for  $i_t = 5^\circ$ .



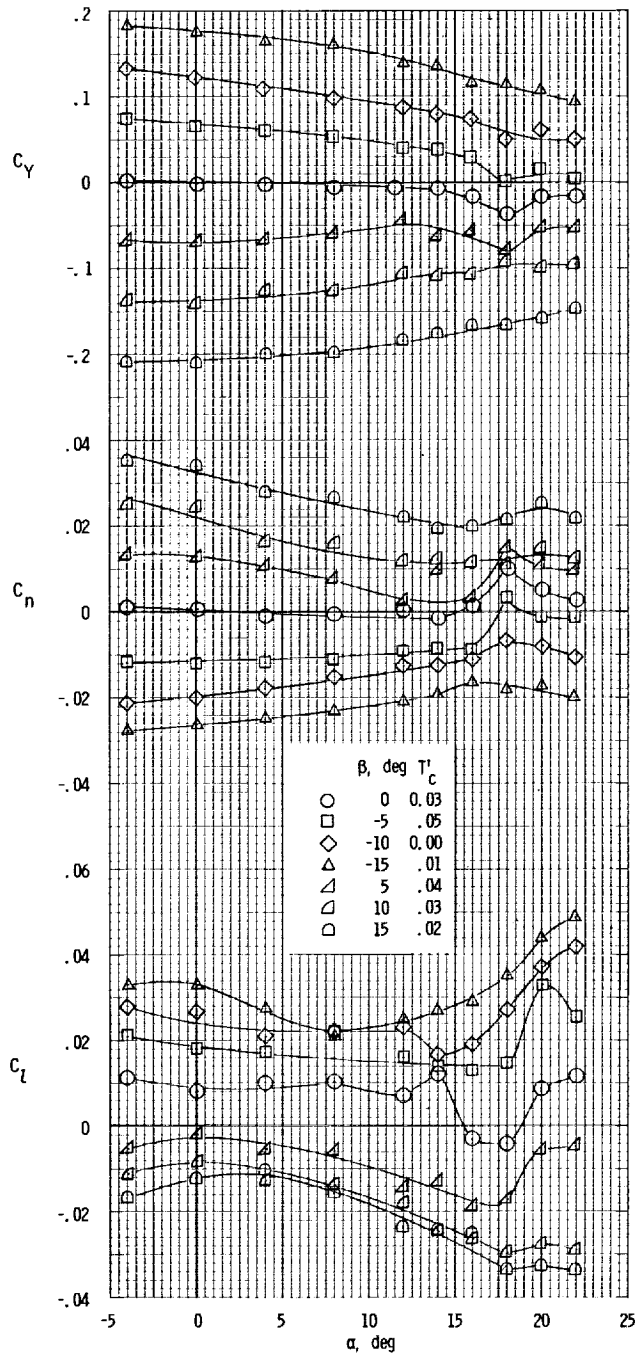
(b)  $\delta_f = 20^\circ$ .

Figure 14.- Continued.



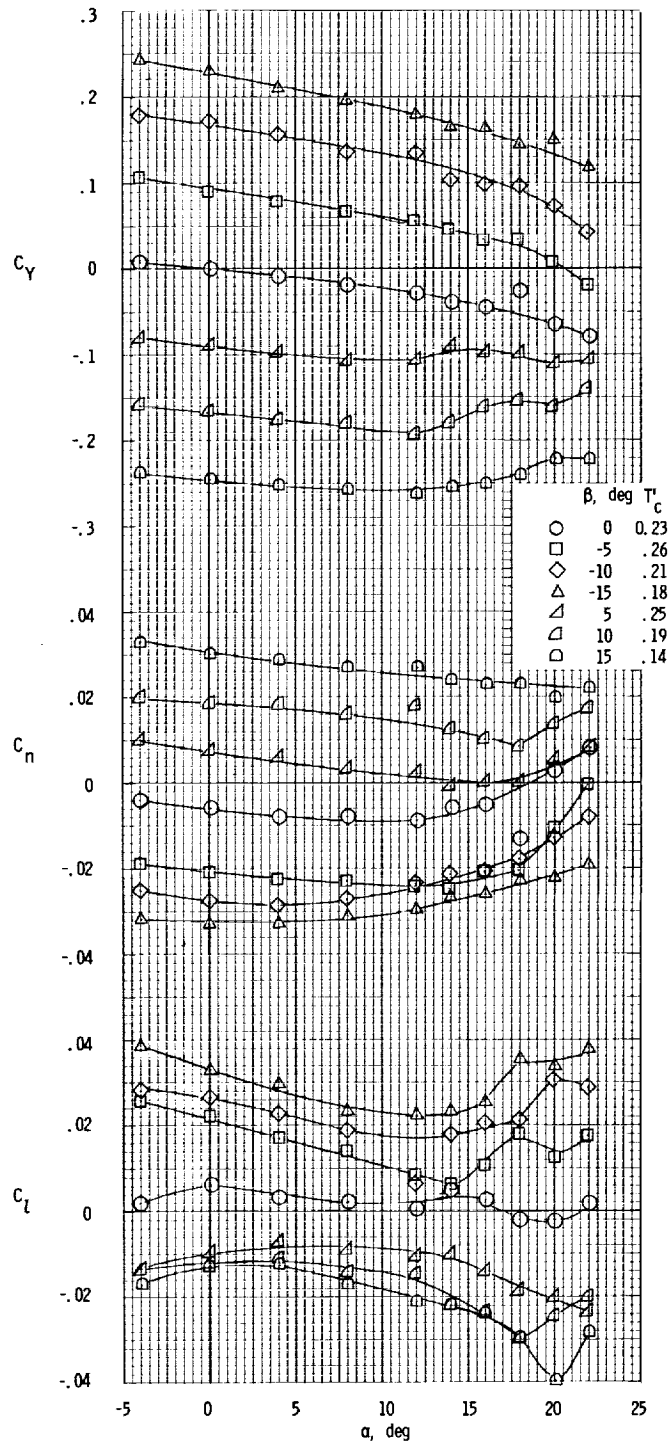
(c)  $\delta_f = 30^\circ$ .

Figure 14.- Concluded.



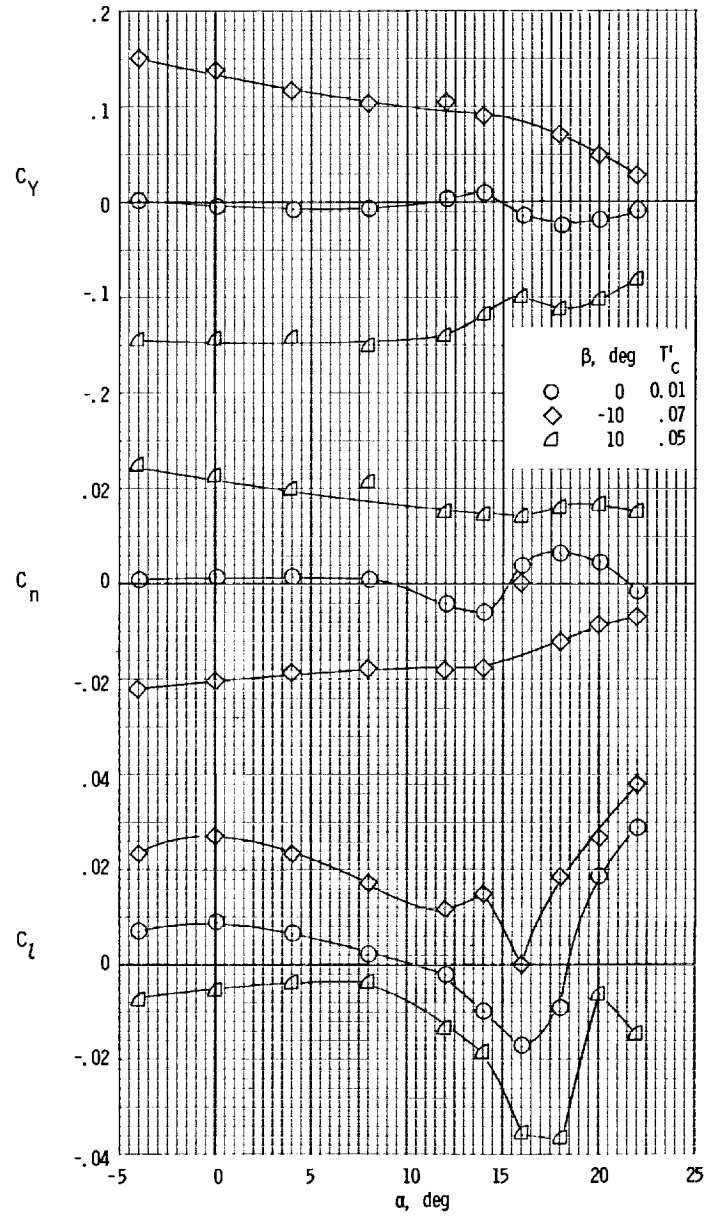
(a)  $T'_c \approx 0.03$ .

Figure 15.- Lateral stability and control characteristics of the airplane for several sideslip angles and thrust coefficients for  $\delta_f = 0^\circ$ .



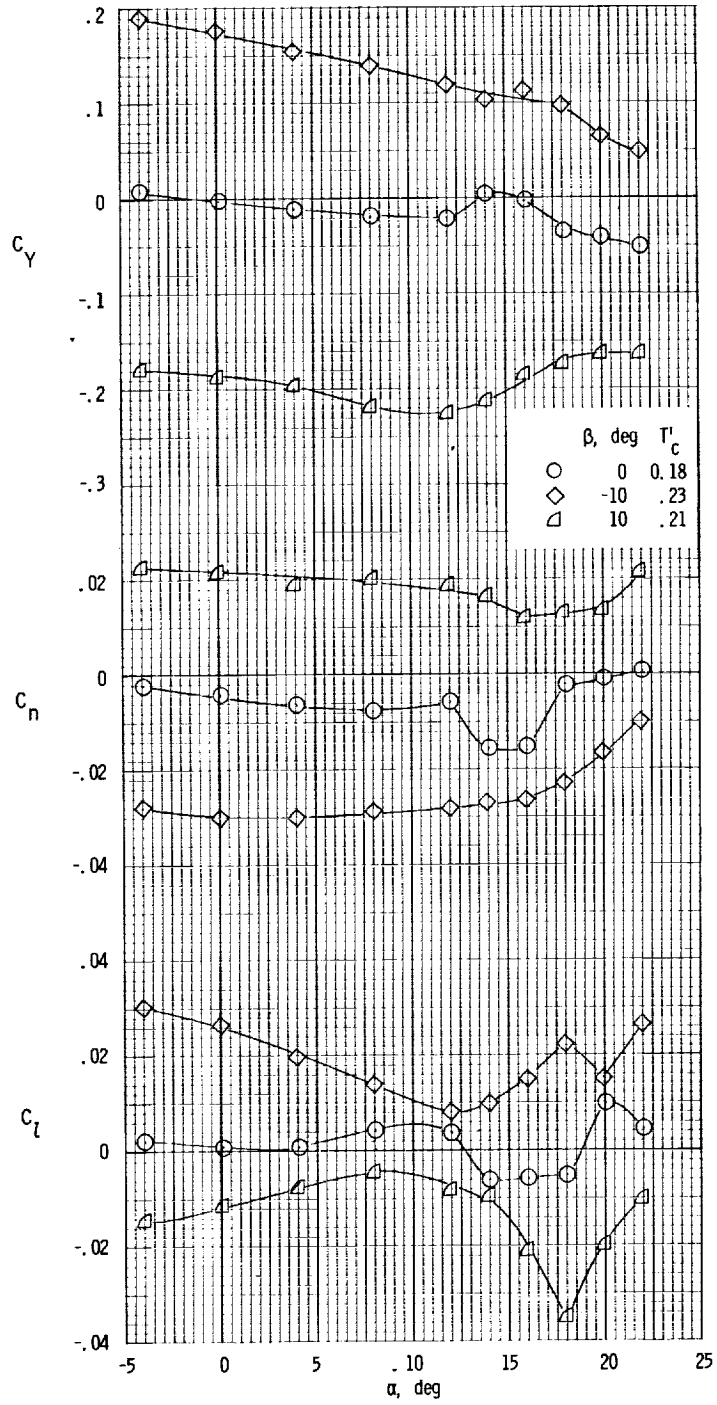
(b)  $T_c \approx 0.20$ .

Figure 15.- Concluded.



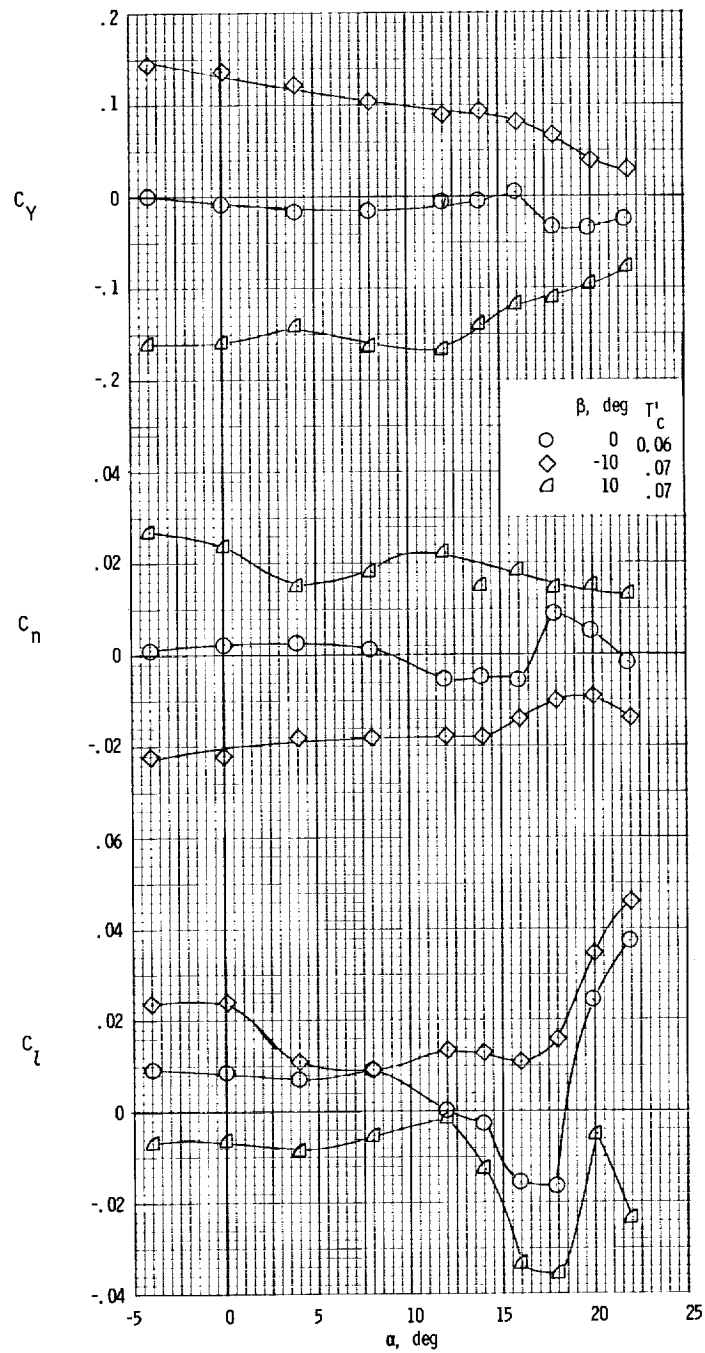
(a)  $T'_C \approx 0.04$ .

Figure 16.- Lateral stability and control characteristics of the airplane for several sideslip angles and thrust coefficients for  $\delta_f = 20^\circ$ .



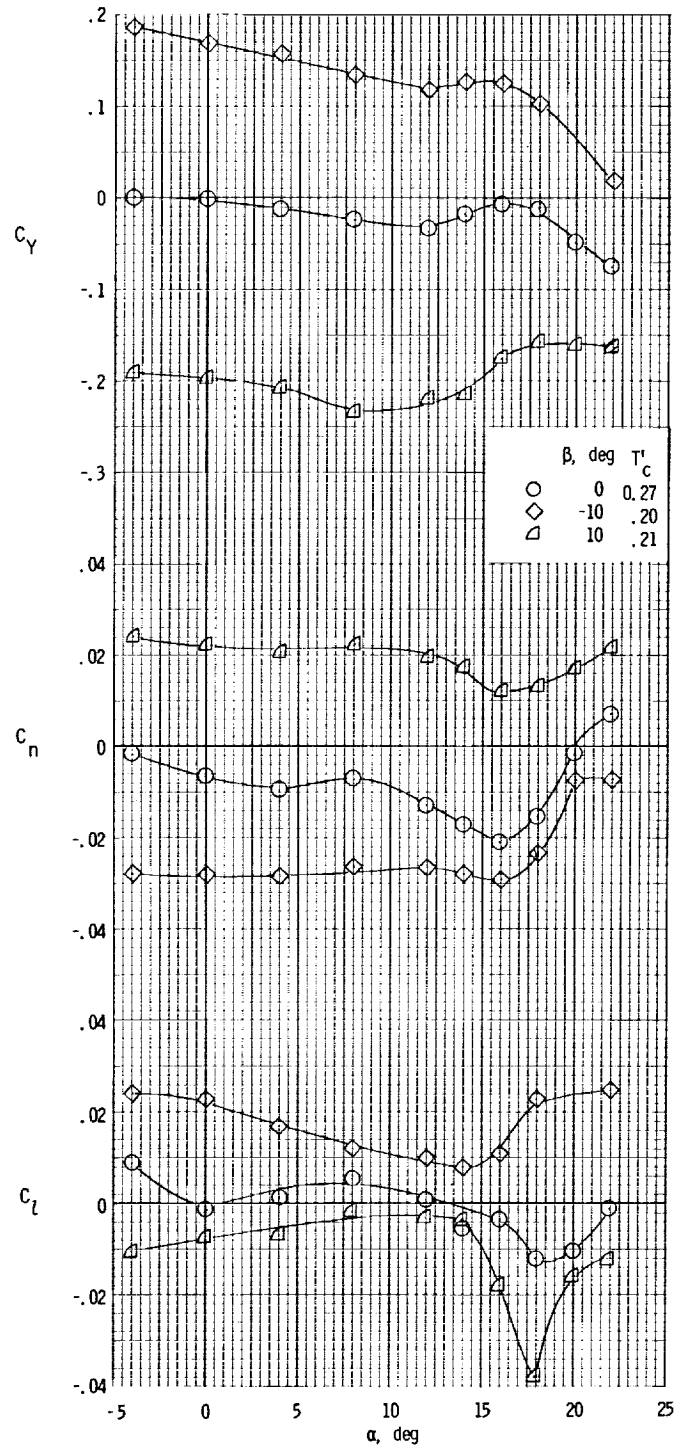
(b)  $T_c \approx 0.20$ .

Figure 16.- Concluded.



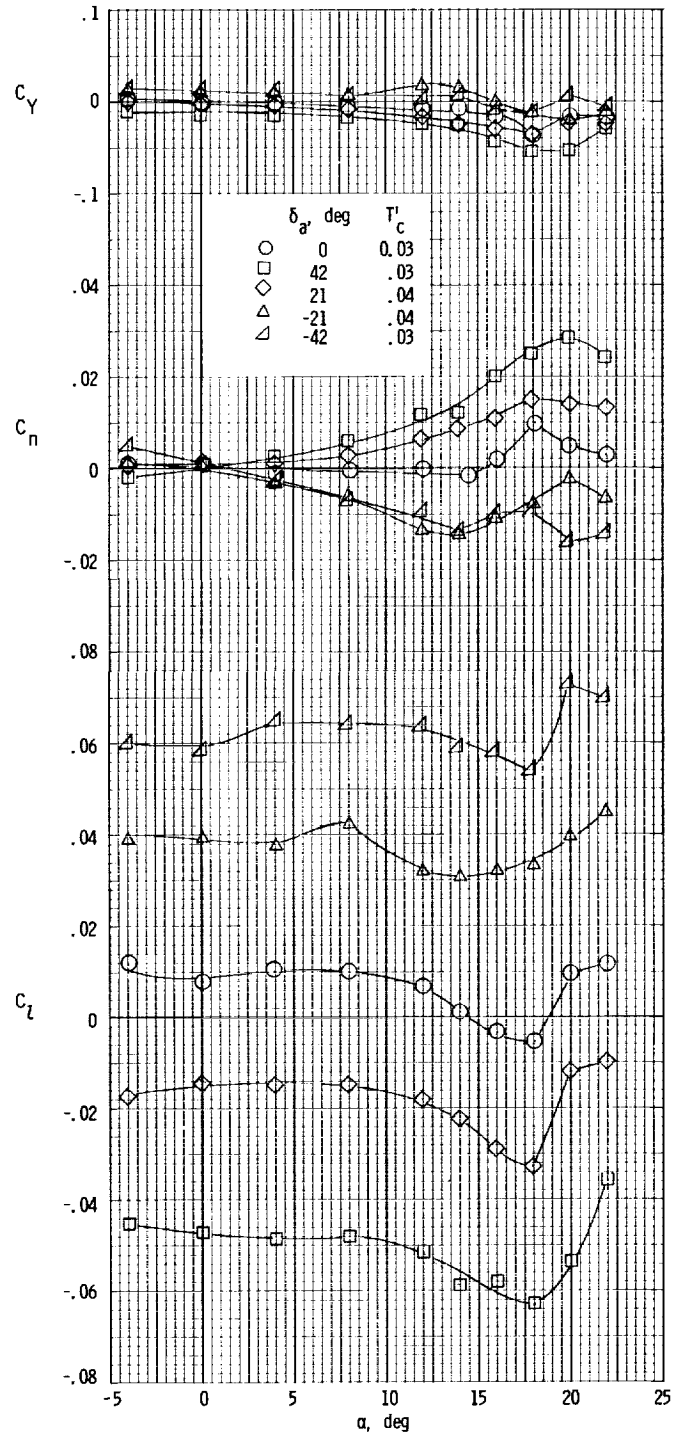
(a)  $T'_c \approx 0.07$ .

Figure 17.- Lateral stability and control characteristics of the airplane for several sideslip angles and thrust coefficients for  $\delta_f = 30^\circ$ .



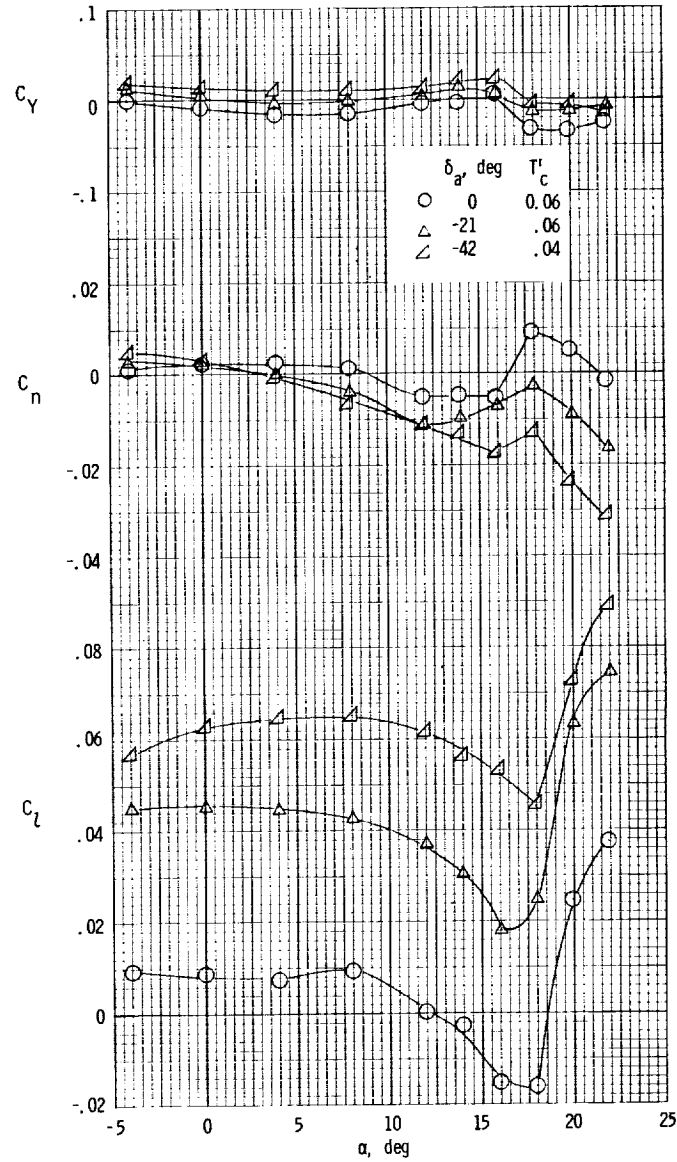
(b)  $T_c \approx 0.23$ .

Figure 17.- Concluded.



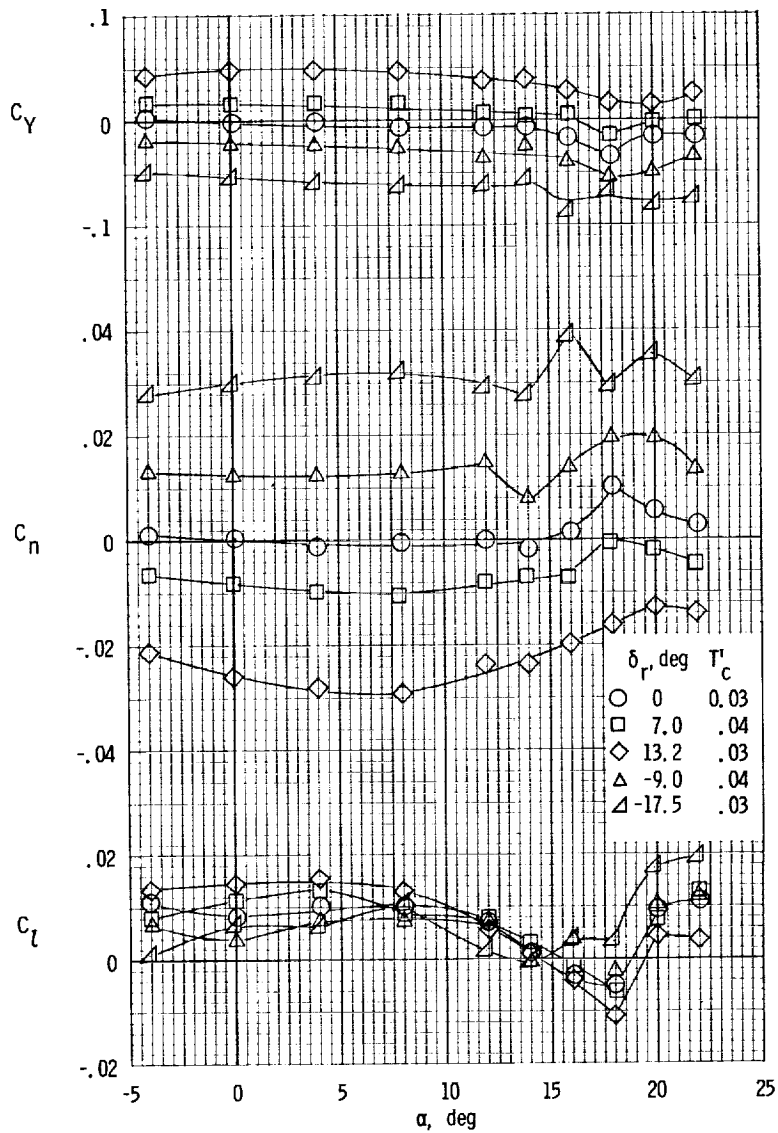
(a)  $\delta_f = 0^\circ$ .

Figure 18.- Variation of the lateral stability and control characteristics of the airplane with angle of attack for several aileron deflections and flap deflections.  $\beta = 0^\circ$ .



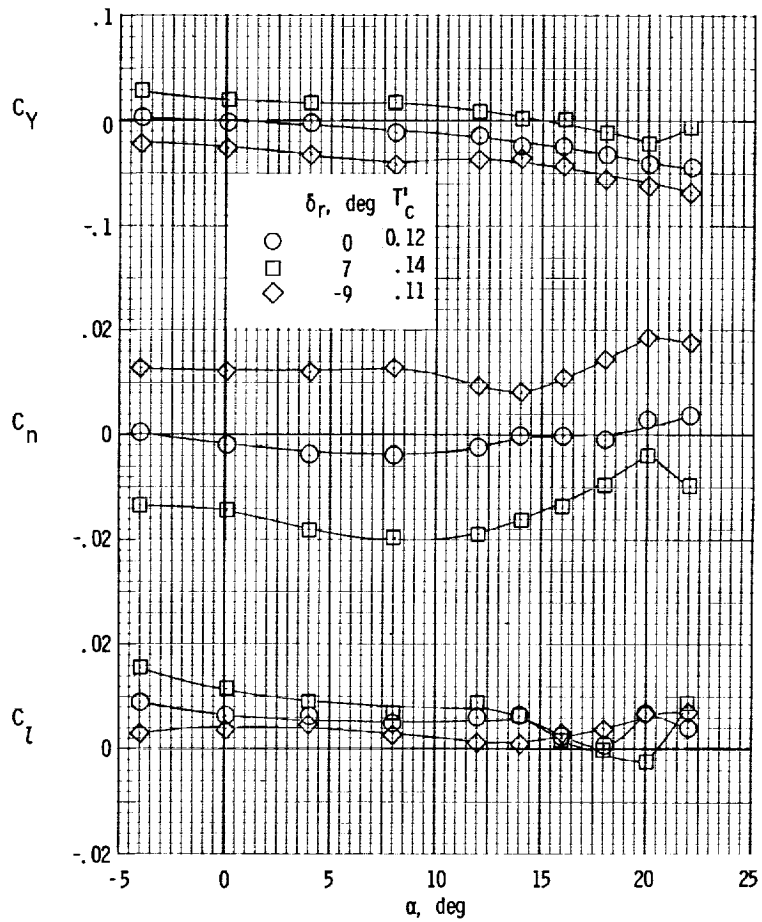
(b)  $\delta_f = 30^\circ$ .

Figure 18.- Concluded.



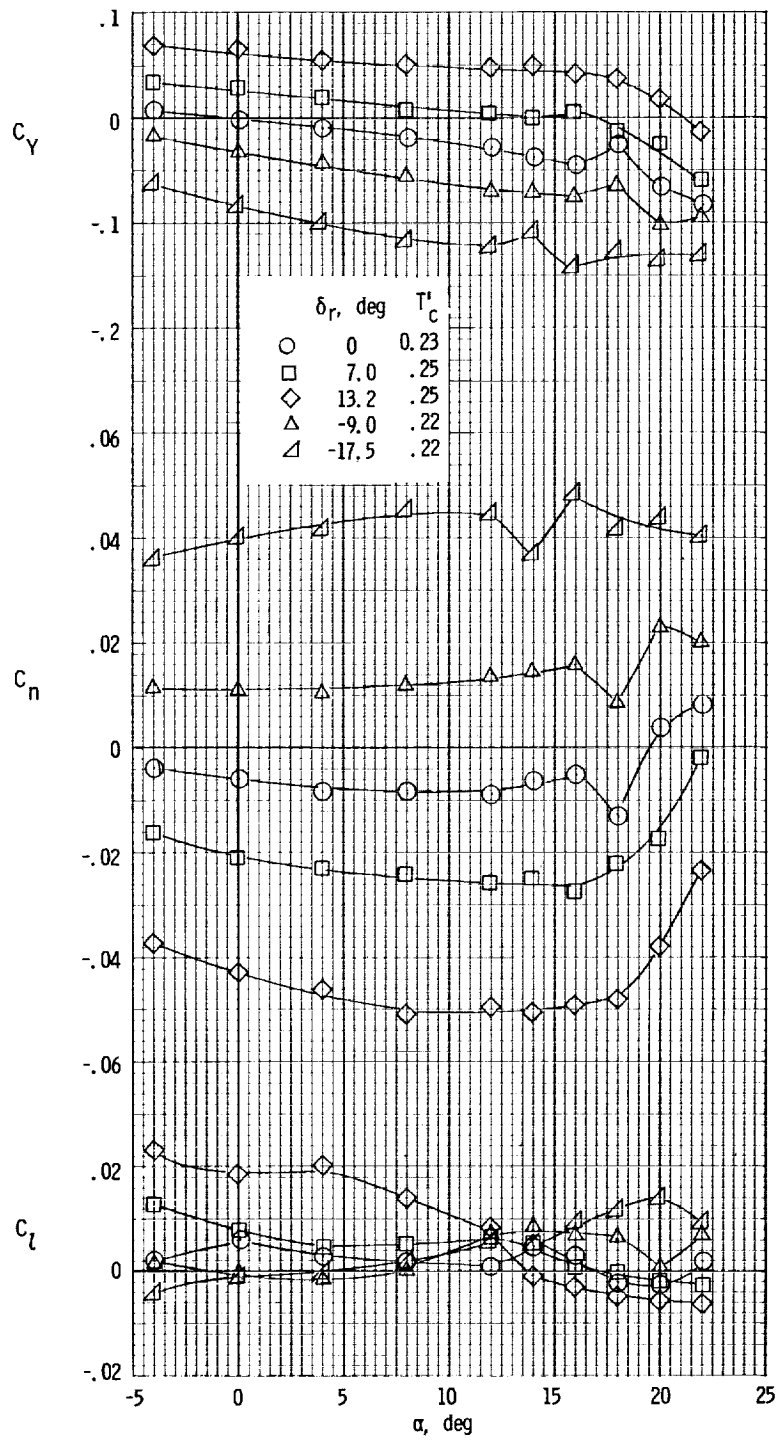
(a)  $T'_c \approx 0.03$ .

Figure 19.- Variation of the lateral stability and control characteristics of the airplane with angle of attack for several rudder deflections and thrust coefficients for  $\delta_f = 0^\circ$  and  $\beta = 0^\circ$ .



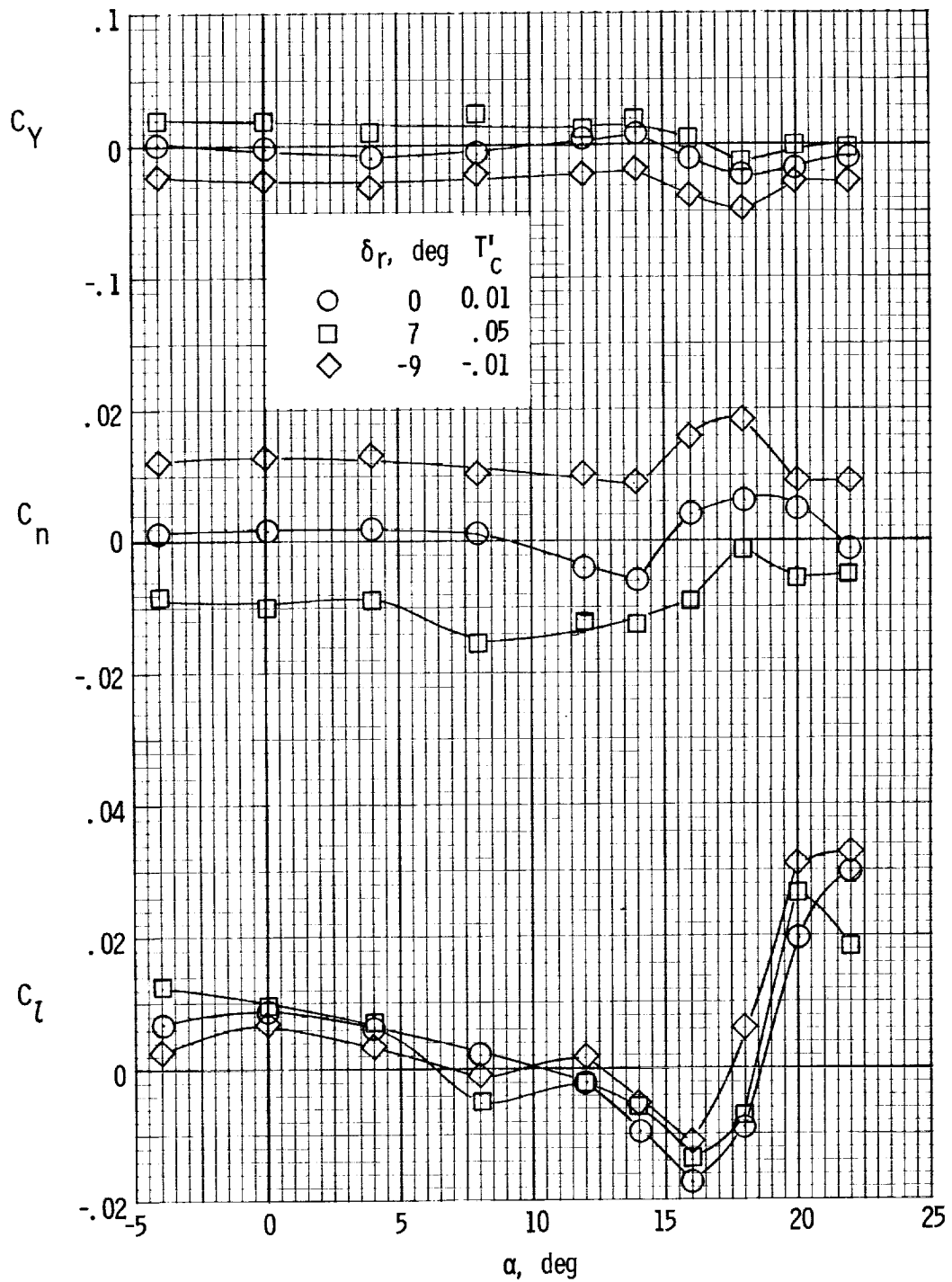
(b)  $T_c \approx 0.12$ .

Figure 19.- Continued.



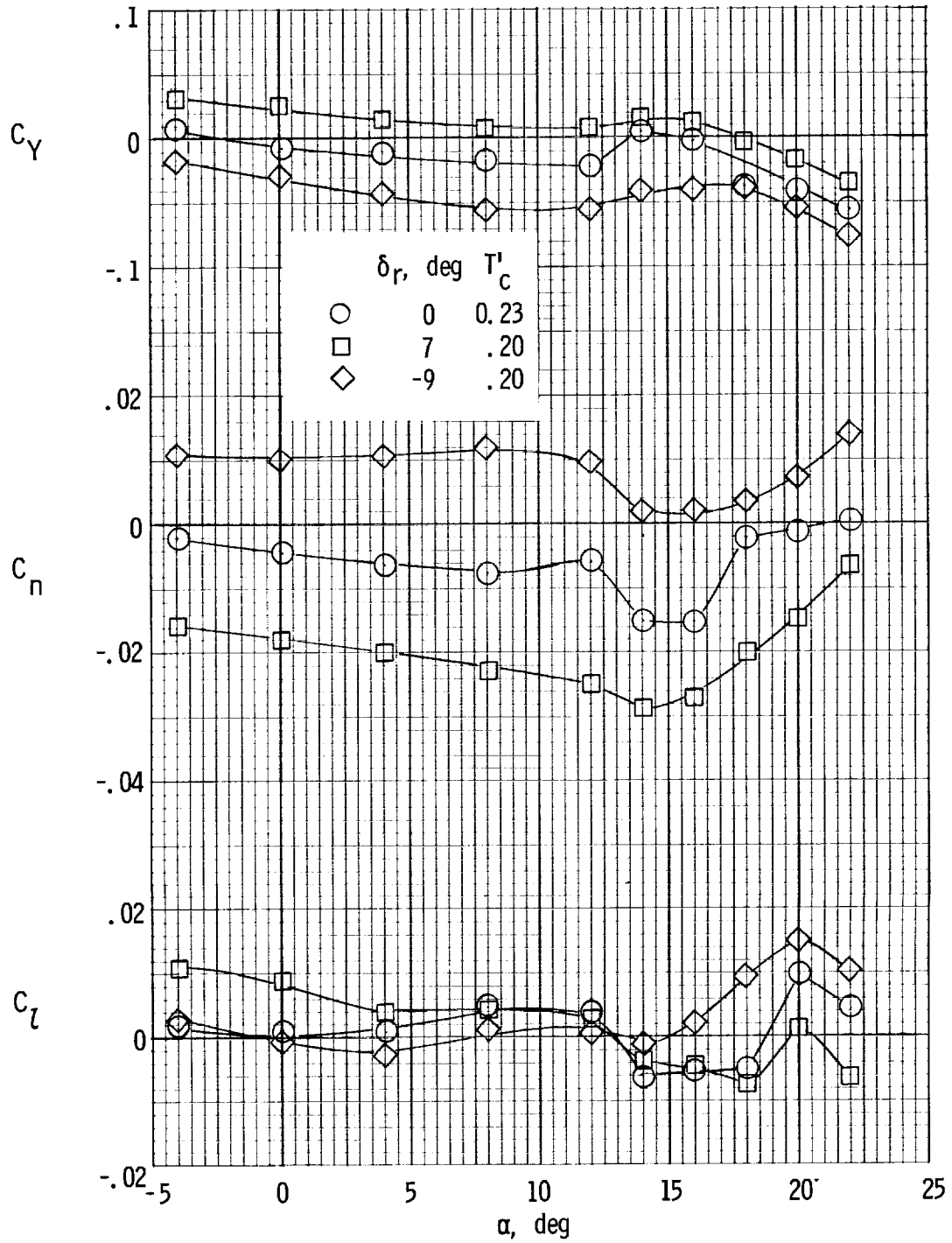
(c)  $T'_c \approx 0.23$ .

Figure 19.- Concluded.



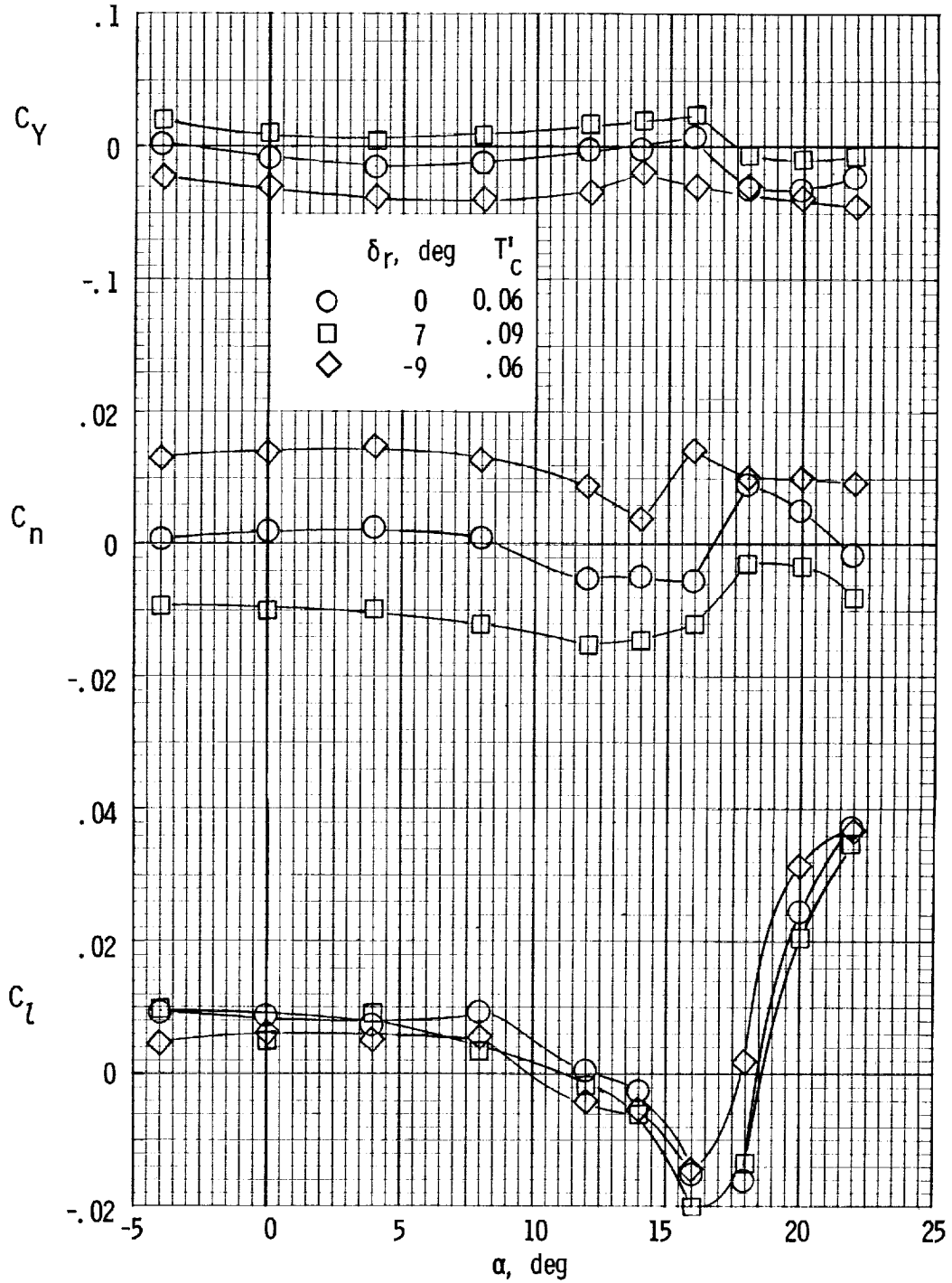
(a)  $T'_c \approx 0$ .

Figure 20.- Variation of the lateral stability and control characteristics of the airplane with angle of attack for several rudder deflections and thrust coefficients for  $\delta_f = 20^\circ$  and  $\beta = 0^\circ$ .



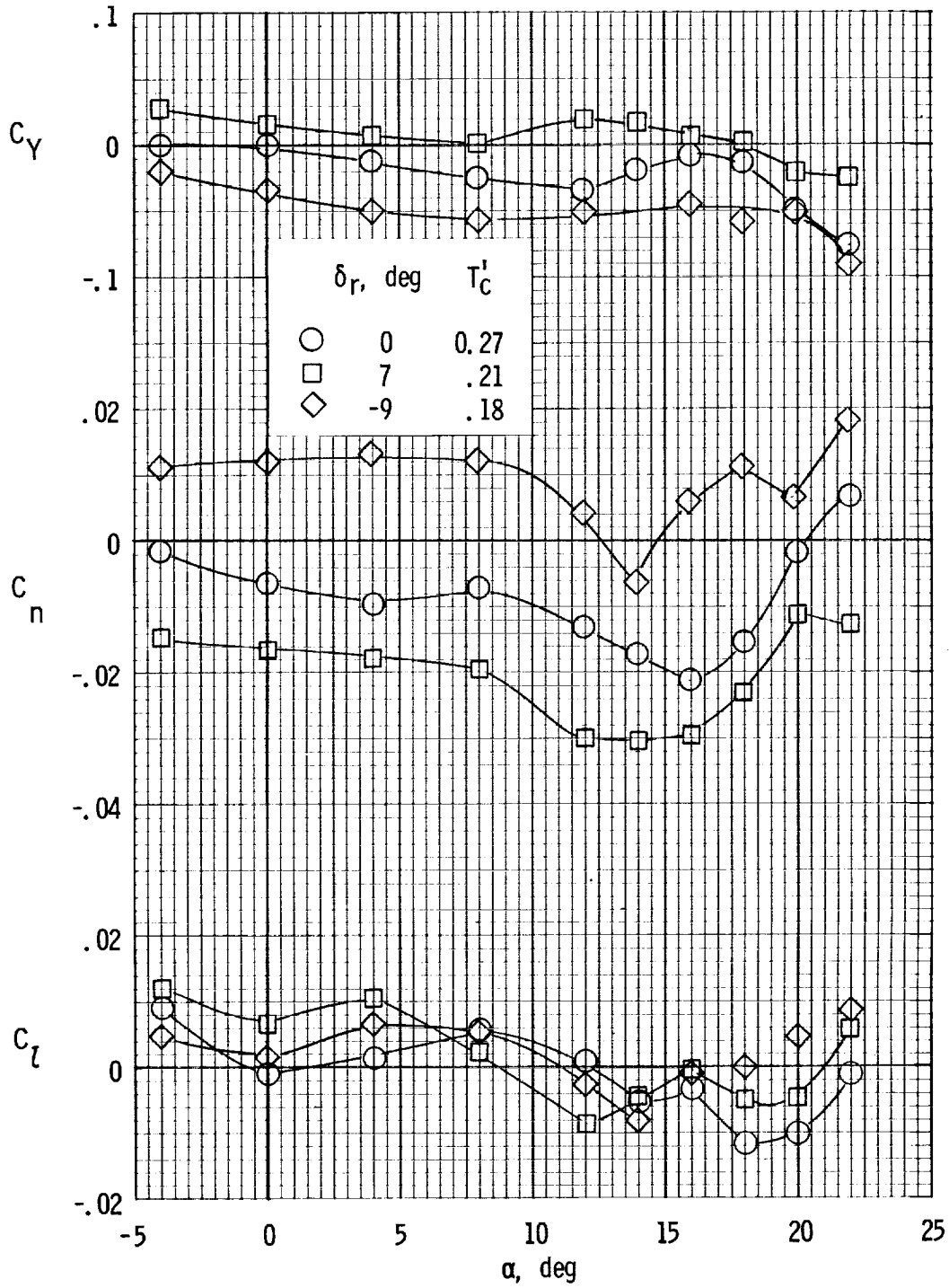
(b)  $T'_c \approx 0.20$ .

Figure 20.- Concluded.



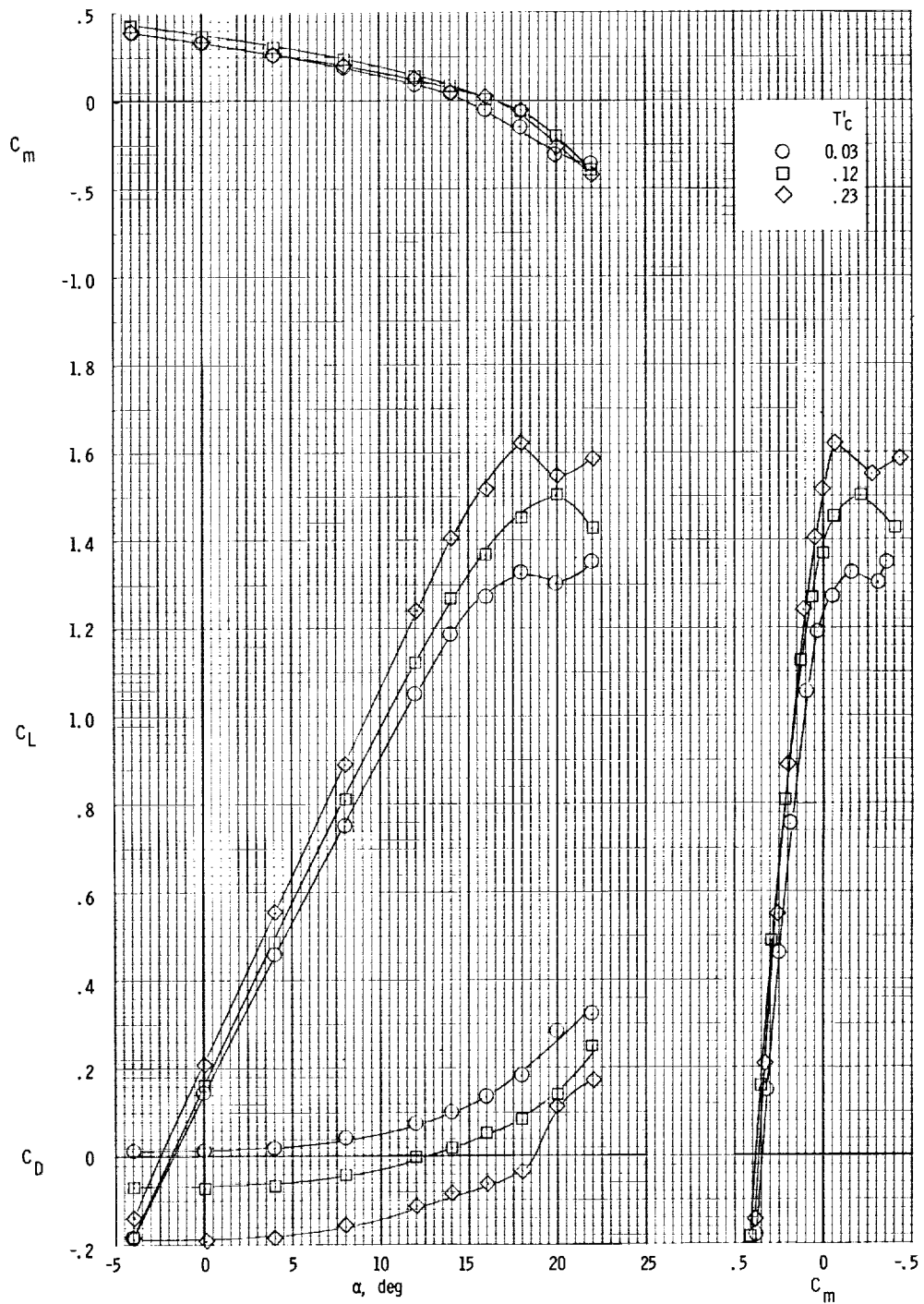
(a)  $T'_c \approx 0.07$ .

Figure 21.- Variation of the lateral stability and control characteristics of the airplane with angle of attack for several rudder deflections and thrust coefficients for  $\delta_r = 30^\circ$  and  $\beta = 0^\circ$ .



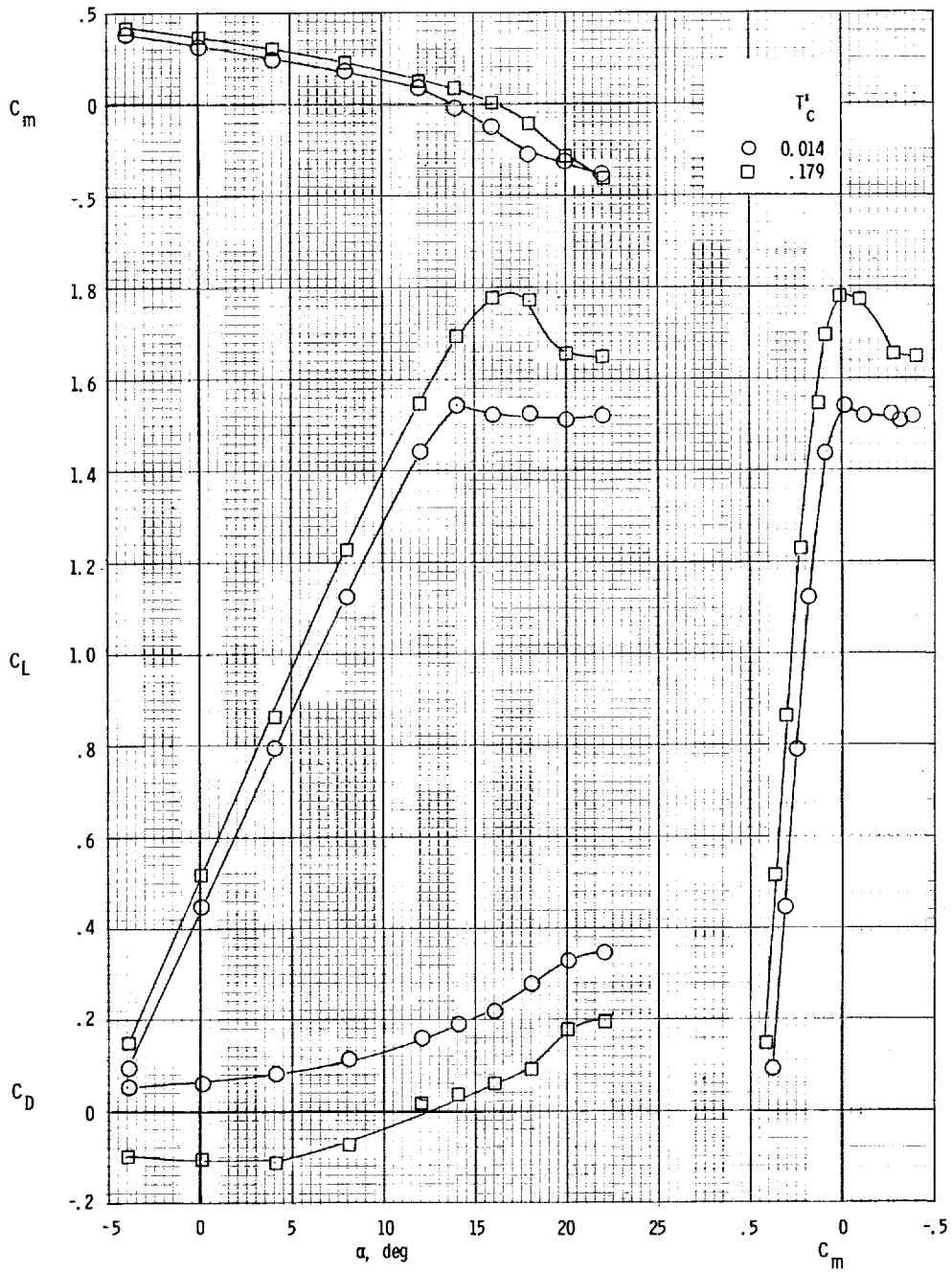
(b)  $T_c^i \approx 0.23$ .

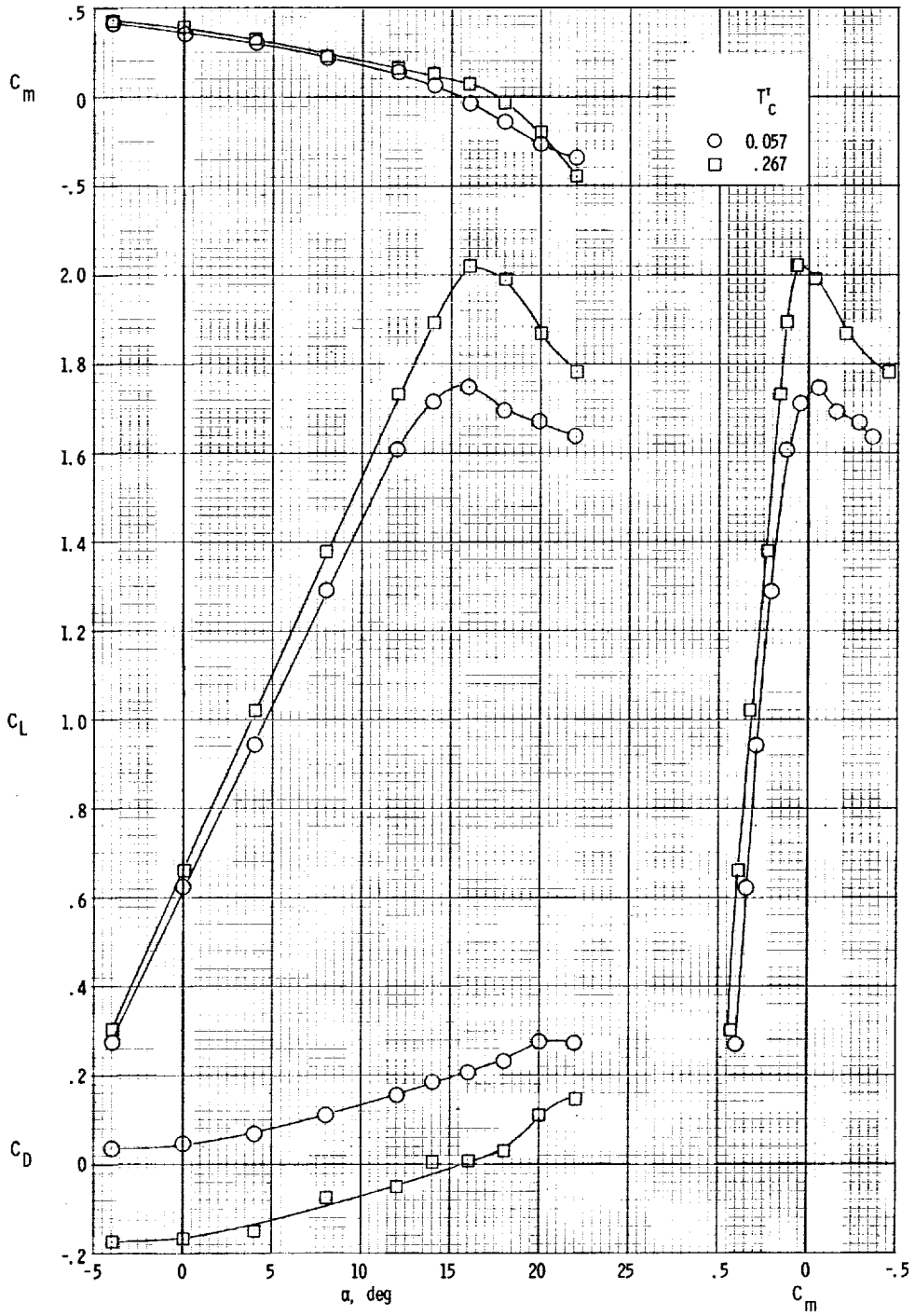
Figure 21.- Concluded.



(a)  $\delta_f = 0^\circ$ .

Figure 22.- Effect of power on longitudinal aerodynamic characteristics.  $i_t = -5^\circ$ .





(c)  $\delta_f = 30^\circ$ .

Figure 22.- Concluded.

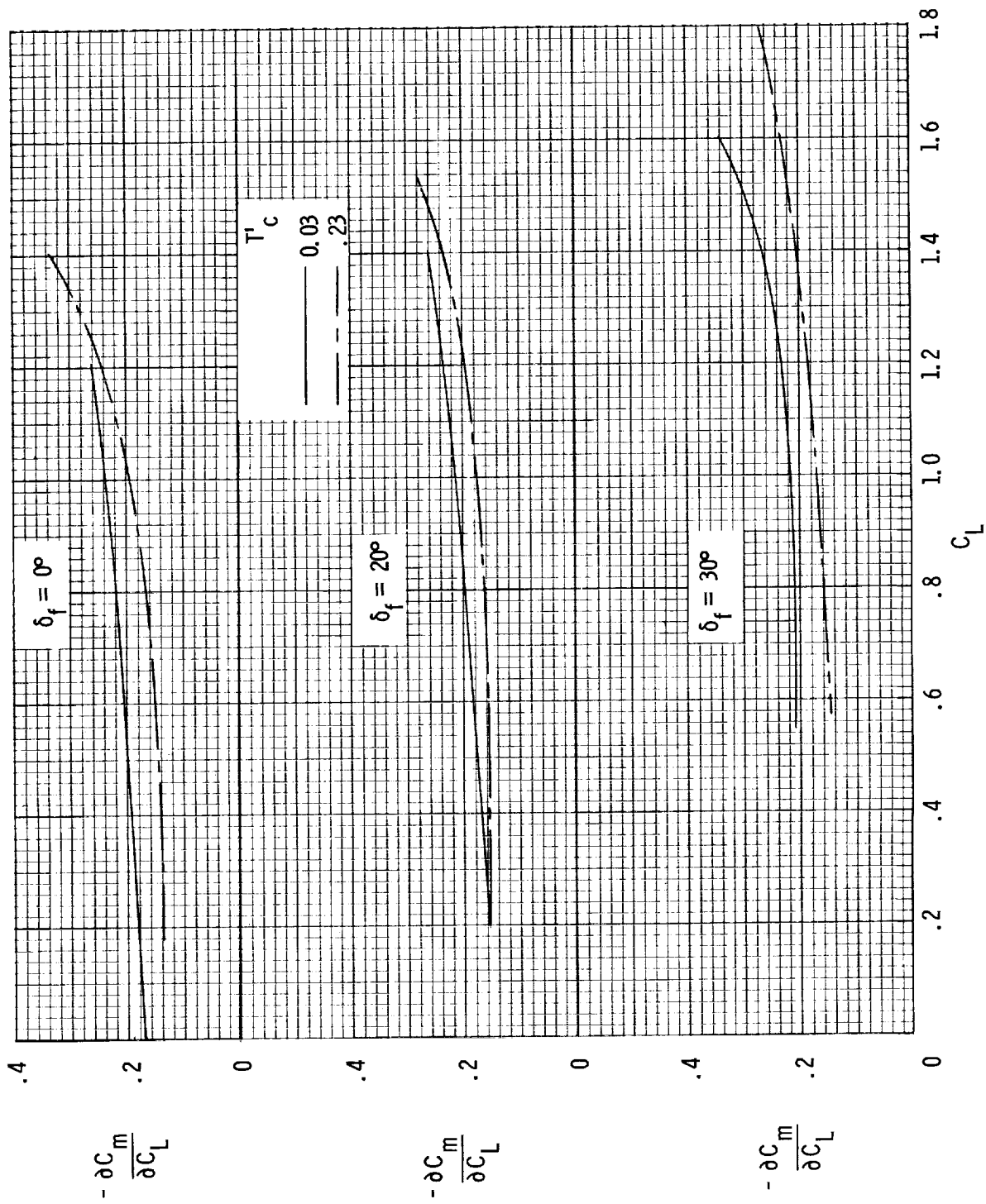


Figure 23.- Variation of the static longitudinal stability with lift coefficient for several thrust coefficients and flap deflections.  $i_t = -5^\circ$ .

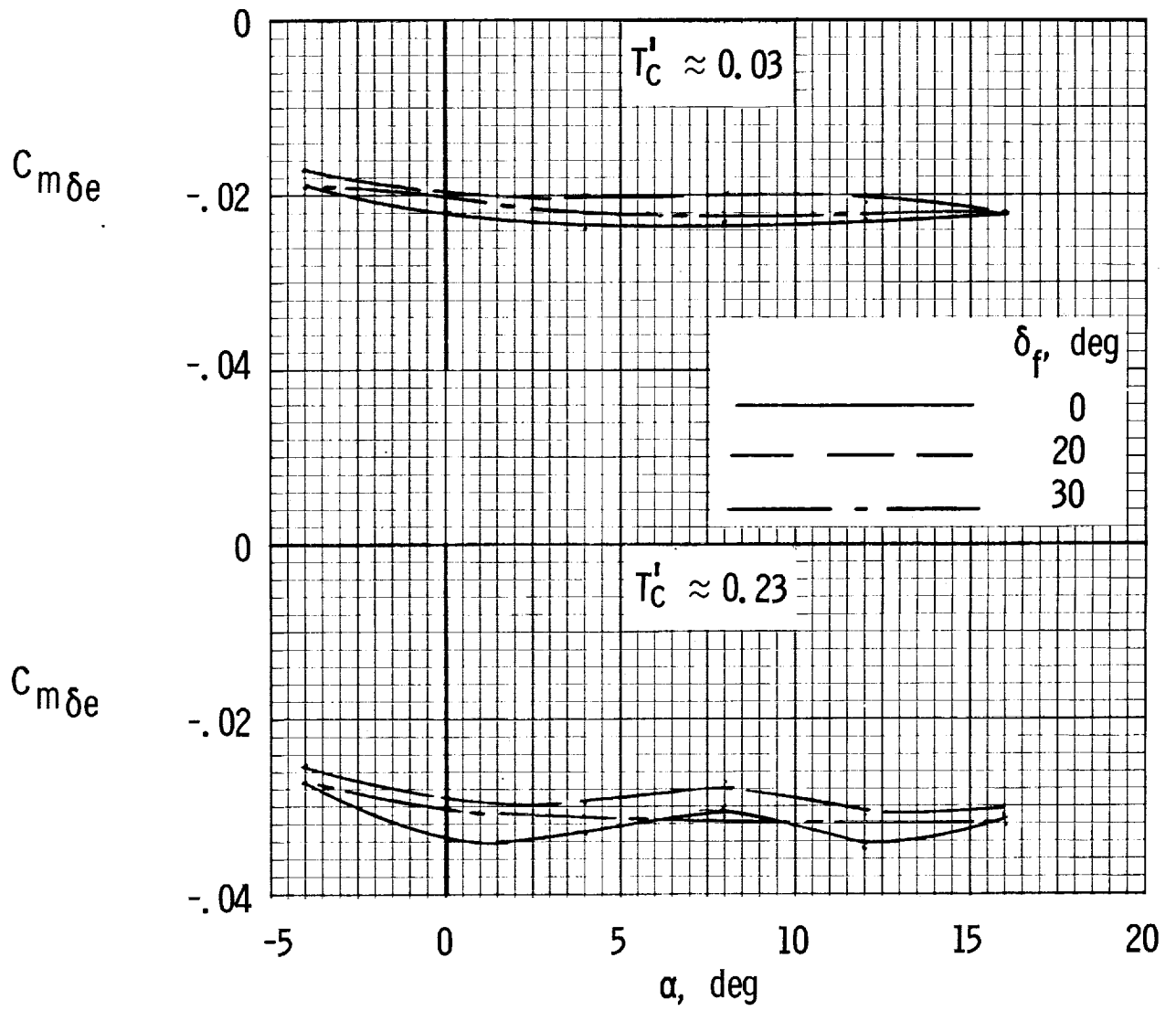


Figure 24.- Variation of elevator effectiveness with angle of attack.  $i_t = -5^\circ$ .

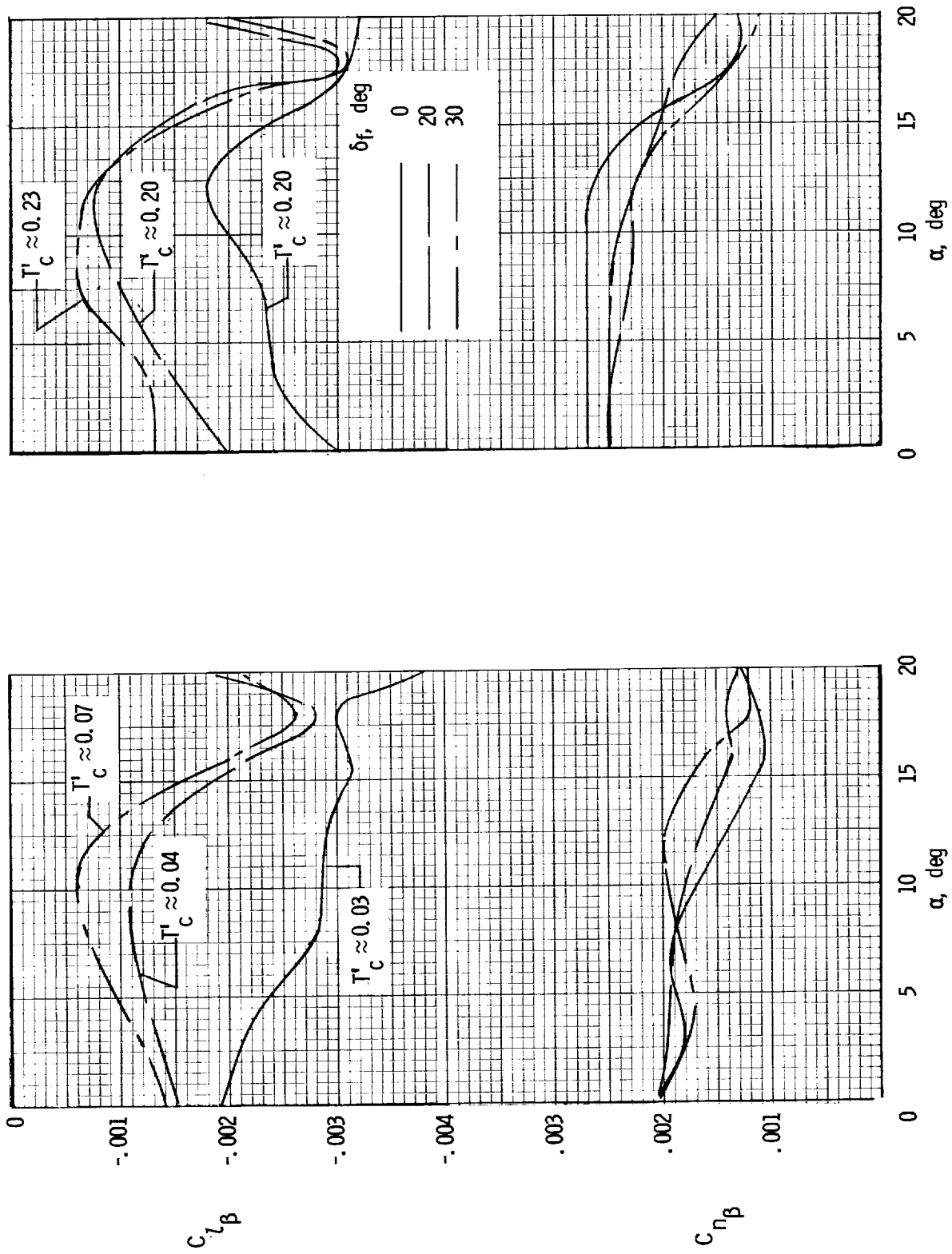


Figure 25.- Effective dihedral and directional stability characteristics.

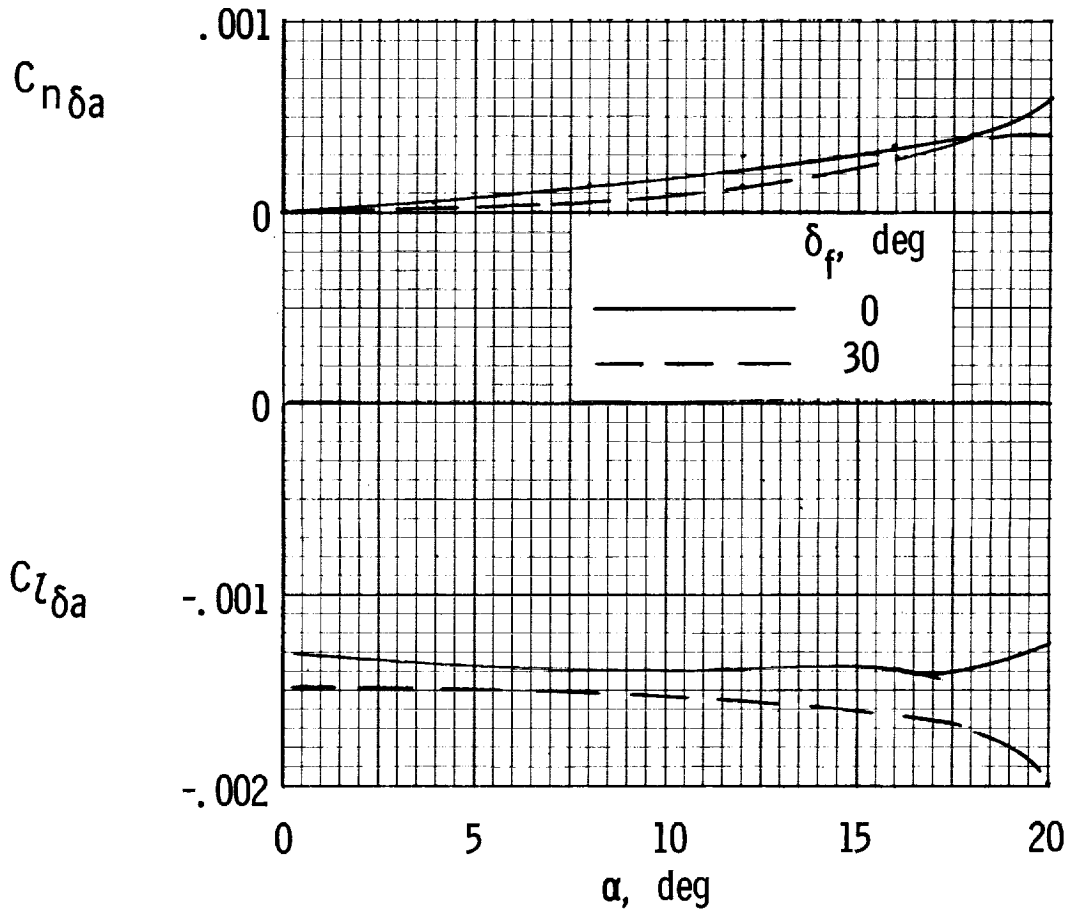


Figure 26.- Variation of aileron rolling- and yawing-moment parameters with angle of attack for several flap deflections.  $T_c^1 \approx 0.03$ .

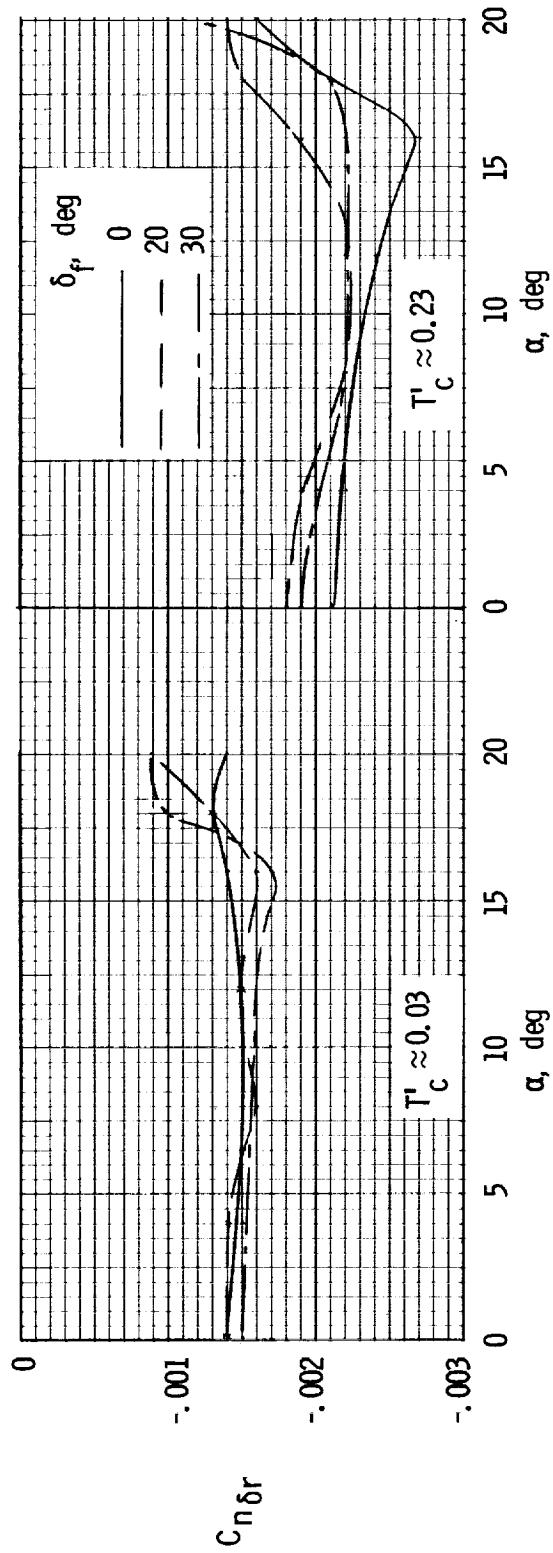


Figure 27.- Variation of rudder effectiveness parameter with angle of attack for several flap deflections and thrust coefficients.

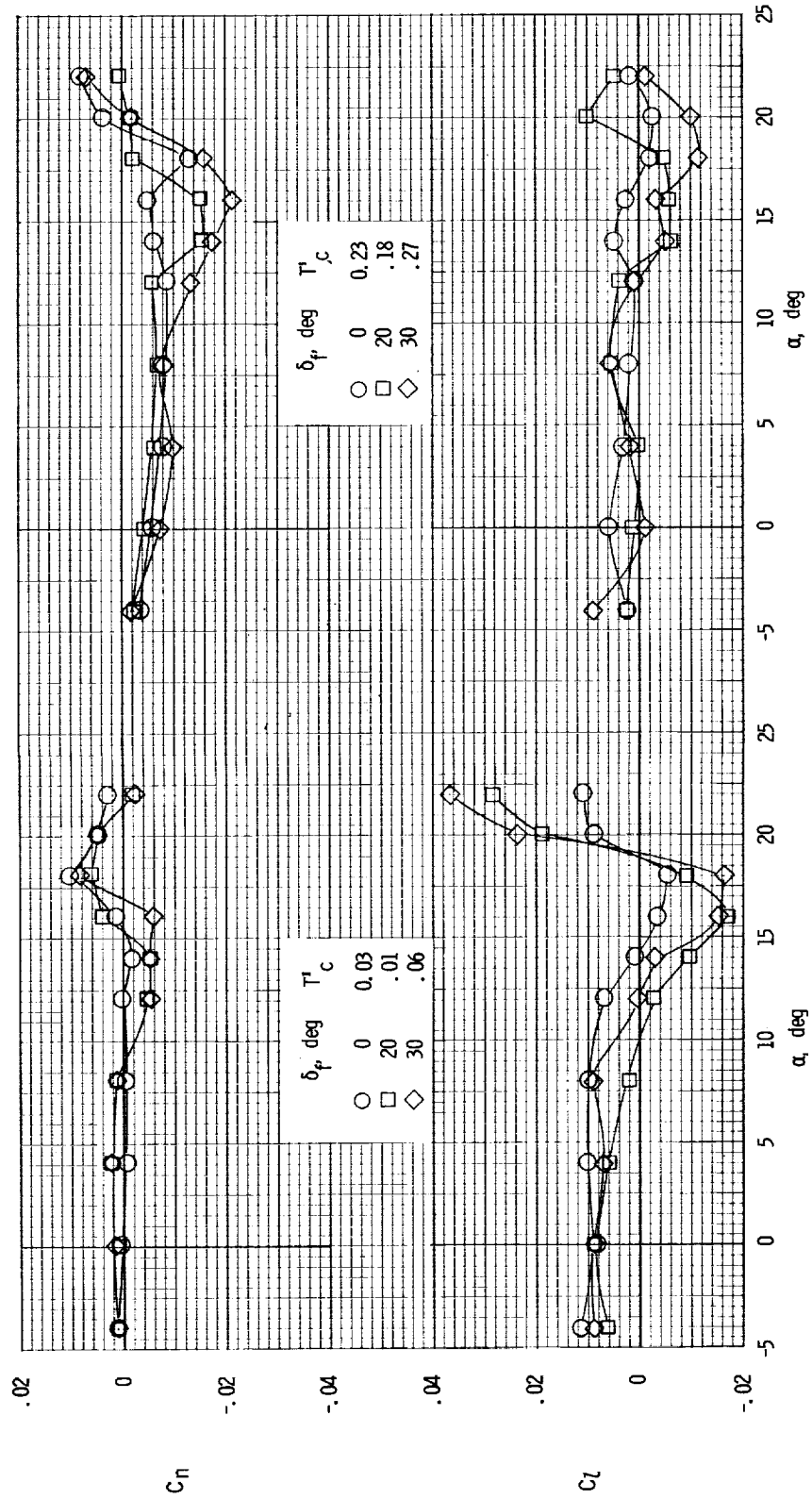


Figure 28.- Variation of rolling- and yawing-moment coefficients with angle of attack.  $\beta = 0^\circ$ .

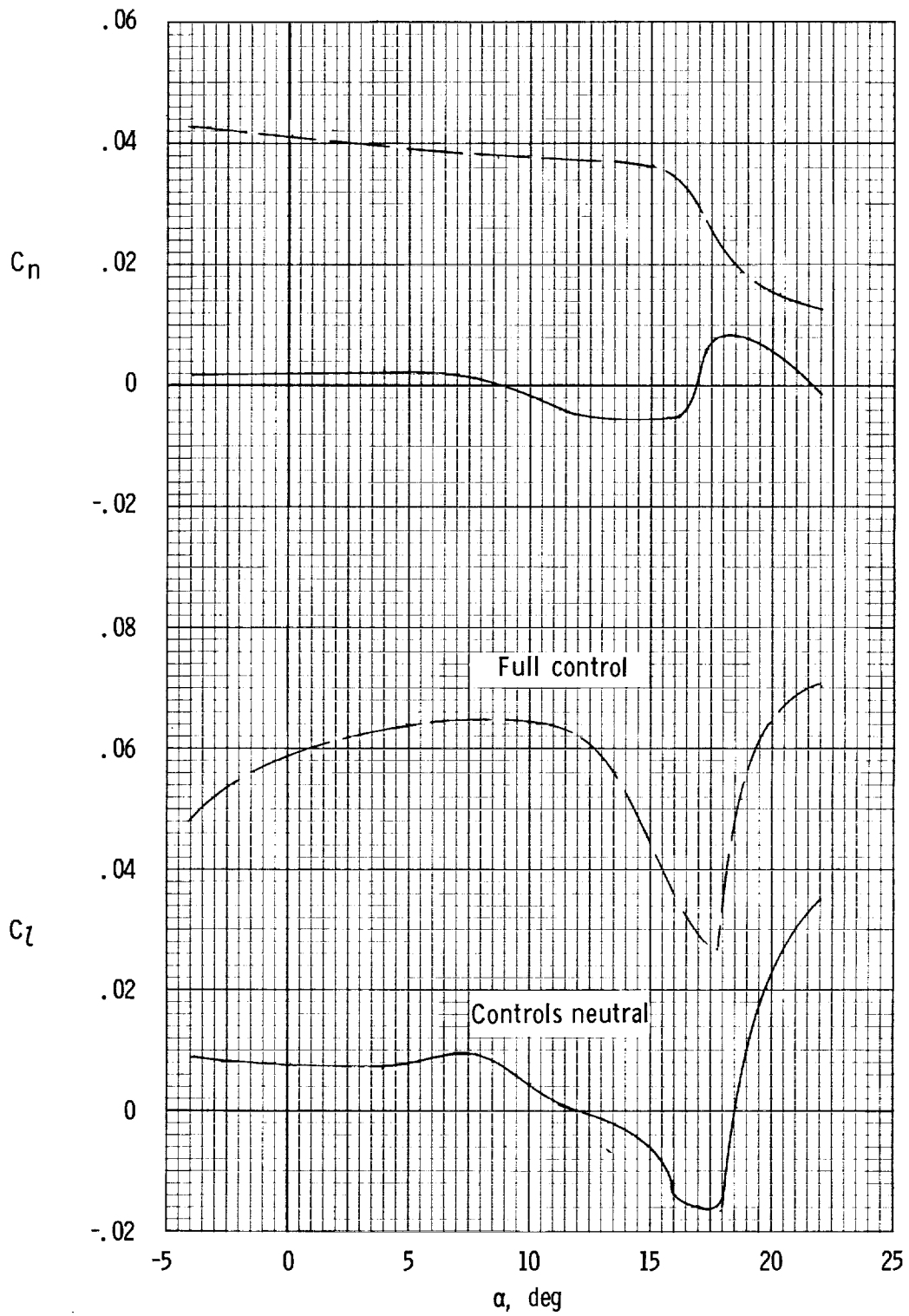


Figure 29.- Control capability for overcoming lateral moment.  $T_C' \approx 0.03$ ;  $\delta_f = 30^\circ$ ;  $\beta = 0^\circ$ .

